

RETURNING MATERIALS: Place in book drop to

remove this checkout from your record. FINES will be charged if book is returned after the date stamped below.

EXPERIMENTAL INVESTIGATION

of a

COANDA JET

Ву

William Charles Oakes

A THESIS

Submitted to
Michigan State University
in partial fulfillment of the requirements
for the degree of

MASTER OF SCIENCE

Department of Mechanical Engineering

1987

ABSTRACT

EXPERIMENTAL INVESTIGATION OF A COANDA JET

BY

William Charles Oakes

A nonisothermal, coanda jet was examined as part of a larger investigation of room air distributions in indoor swimming pools.

Velocity, temperature and water vapor concentration values were recorded in the separated and reattaching region of the jet as well as reattachment lengths. Parameters of inlet temperature and velocity, reattaching wall temperature and geometries of jet width, distance to wall and angle of jet were varied.

Geometry was found to be the determining factor for the overall flow characteristics. Some effects of buoyancy were observed for Re less than 4000. Ambient currents in the measurement chamber were found to increase reattachment lengths. Comparison with the computer model shows a momentum deficit within two reattachment lengths of the jet inlet.

LEHRSTUHL FÜR WÄRMEÜBERTRAGUNG UND KLIMATECHNIK RHEINISCH-WESTFÄLISCHE TECHNISCHE HOCHSCHULE AACHEN PROFESSOR DR.-ING. U. RENZ

Masters Thesis for Herrn William C. Oakes, Matr.-Nr. 154390

Theme:

Experimental investigation of a two-dimensional, buoyant coanda jet and redeveloped wall jet with comparison to computer predictions

Aachen, 10. September 1986

(Prof. Dr.-Ing. U. Renz)

Acknowledgements

I would like to thank Dipl.-Ing. Jürgen Ahl for his guidance and assistance in completing my work. His extra efforts to make my stay in Germany enjoyable have been greatly appreciated. I wish to acknowledge Prof. J. Foss who arranged for my project and provided valuable advice and assistance. I am grateful to Prof. U. Renz and Prof. J. Lloyd who gave me the opportunity to do my masters thesis at RWTH Aachen. I also wish to thank Prof. B. Thompson for his efforts during the first few months in Aachen.

I would like to gratefully acknowledge Frau Fengels and Akademisches Auslandsamt for their help and support through my stipend from the state of Nordrhein-Westfalen.

A special thanks goes to Rolf, Hartmut and everyone at Lehrstuhl für Wärmeübertragung und Klimatechnik who helped make my stay in Aachen something which I will always remember.

Finally, I wish to express my appreciation to Kristin and my family for their support from home which made the difficult times much easier to overcome.

TABLE OF CONTENTS

List of Tablesvii
List of Figuresviii
Nomenclatureix
1. Introduction
2. Literature Review
3. Computer Program6
4. Equipment and Procedure
5. Results and Discussion18
5.1 Documentation of the jet18
5.2 Separated and reattaching zone24
5.2.1 Reattachment lengths24
5.2.2 Velocity and temperature measurements
5.2.3 Change in inlet temperature35
5.2.4 Change in wall temperature37
5.2.5 Change in Reynolds number40
5.2.6 Changes in slot width40
5.2.7 Changes in step height47
5.2.8 Changes in jet angle50
5.2.9 Water vapor concentration measurements52
5.3 Comparison with computer predictions54
5.3.1 Reattachment lengths55
5.3.2 Comparison of velocity profiles57

5.4 Wall jet region	. 62
6. Conclusions	. 67
Appendix A (Measurement grids)	.70
Appendix B (Measured data)	. 77
References	82

LIST OF TABLES

Number	Description	Page
1	Reattachment lengths along jet	20
2	Room and wall temperatures	33
3	Reattachment lengths, measured and predicted	56
4	Comparison of velocity magnitudes	60
5	Inlet velocity profiles	81
6	2-D checks for velocity and temperature	82
7	Measurements at grid locations	83
8	Wall jet measurements	85

LIST OF FIGURES

Number	Description	Page
1	Flow pattern of measurement chamber	.10
2	Jet inlet structure	.12
3	Reattachment flags	.13
4	Reattachment flags	.14
5	Measurement robot and flags	.14
6	Grid measurement robot	.16
7	Room measurement robot	.16
8	Measurement locations	.17
9	Inlet velocity profiles	.19
10	Velocity and temperature profiles at the	
	jet inlet	.21
11	Velocity and temperature profiles at 0.5 L	.22
12	Velocity and temperature profiles at 2 L	.23
13	Reattachment lengths	.25
14	Comparison of reattachment lengths with	
	Regenscheit /4/	.26
15	Room currents running parallel to the jet	.27
16	Analysis of Sawyer /3/	.28
17	Computed velocity profiles showing an area	
	of negative u components	.29
18	Possible flow patterns for negative u	
	velocity components	.30
19	Velocity and temperature profiles together	.34
20	Velocity profiles for change in inlet	
	temperature	.36
21	Velocity profiles for change in wall setting	.38
22	Temperature profile for change in wall setting	.39

23	Source of temperature discrepancy for d/w=17.5.39
24	Velocity profiles for change in Re41
25	Velocity profiles for change in slot width42
26	Universal velocity profile44
27	Universal temperature profiles45
28	Isothermal and nonisothermal velocity profiles.46
29	Velocity profiles at different step heights48
30	Velocity profiles at different step heights49
31	Comparison of angle and parallel velocity
	profiles51
32	Water vapor concentration profiles53
33	Measured and computed velocity profiles58
34	Universal velocity profiles, measured and
	computed
35	Developed velocity profiles, measured and
	computed63
36	Universal wall jet profiles for prediction64
37	Wall jet velocity profiles, isothermal and
	nonisothermal66
38	Measurement grid for d/w=574
39	Measurement grid for d/w=1075
40	Measurement grid for d/w=2076
41	Measurement grid for jet at an angle77
42	Measurement grid for d/w=17.578
43	Computational grid79
44	Fine computational grid80

NOMENCLATURE

- C Constant in turbulence model
- d Distance between wall and jet inlet
- E Entrainment parameter for entire jet
- E, Entrainment parameter for wall side of jet
- g Gravity
- G Production or dissipation of turbulent kinetic energy by buoyancy
- h Specific enthalpy
- k Turbulent kinetic energy
- 1 Path length of reattaching streamline from jet inlet to the reattachment point
- L Reattachment length
- p Pressure
- P Production of turbulent kinetic energy
- Pr Prandtl number
- Re Reynolds number based on jet width
- Sc Schmidt number
- T Temperature
- $\Delta T T T_a$
- $\Delta T_{m} T_{i} T_{a}$
- u Velocity component in the x direction
- U Velocity
- v Velocity component in the y direction
- w Jet inlet width
- x Coordinate
- X Grams of water vapor per kg of dry air
- y Coordinate

- α Angle between jet inlet and wall
- δ y position where quantity in 1/2 maximum
- ϵ Dissipation of turbulent kinetic energy
- n Dynamic viscosity
- ξ Mass concentration
- ρ Density
- - Constant in turbulence model

SUBSCRIPTS

- a Ambient
- D Water vapor
- eff- Effective
- i Average inlet condition
- k Kinetic energy
- L Air
- t Turbulent
- w Wall
- ϵ Dissipation

1. INTRODUCTION

A program has been developed by Schmitz /19/ to predict the air movements in an indoor swimming pool. An experimental investigation has been conducted at RWTH Aachen to verify the program. The experimental facility produces a two dimensional condition with a heated pool, a temperature controlled wall to simulate a window exposed to the environment and a wall jet running along this wall to prevent condensation.

The experimental data has shown some discrepancy with the computed results. Specifically, the overall momentum of the room currents is 20-30% lower in the prediction than in the experiments. Differences in temperatures also exist which are believed to be a result of incorrect heat transfer predictions caused by the incorrect velocity fields.

Because the driving force of the room currents is the wall jet, it is suspected that the error occurs in this region. The jet actually issues parallel to, but separated from, the temperature controlled wall. This initial region, where the jet is a coanda jet, is especially of interest because the assumptions of the turbulence model used are not valid. Experimental data giving velocity and temperature profiles do not exist to verify the predicted values in this region.

The present investigation has been undertaken to provide such data to help indentify the areas of discrepancy in the computer program.

2. LITERATURE REVIEW

At present, there appears to be no published literature involving non-isothermal reattaching jets. There is however quite a bit of related work published. Isothermal reattaching jets have been widely studied. Curved mixing layers, which a jet is before reattachment, have been studied for isothermal as well as those cases involving heat transfer. Most of the heat transfer data involving reattaching flows is for sudden enlargements in channels and pipes and for backsteps. All these cases can be applied to the problem under study.

Isothermal reattaching jets have been well documented. Bourque and Newman /1/ examined two geometries of reattaching jets. One involved a plate inclined to the axis of the jet while the other involved a parallel plate offset from the jet axis. Pressure and velocity measurements in the jet and separated regions were made. The reattachment distances were also measured for the different geometries. The measurements were compared with theoretical calculations.

Sawyer /2/ also made velocity and pressure measurements for the case of a jet issuing parallel to a flat plate. His predictions provided reasonable agreement with experiments. He improved on his predictions by including effects of curvature in the jet before reattachment /3/. This included allowing for different rates of entrainment on the two sides of the jet. Using this information, it was possible to produce curves for reattachemnt distances which fit well with existing experimental data.

Experimental investigations showed that before reattachment, the jet behaves much like a free, plane jet. The rate of growth and the velocity profile follow closely with that of a

normal free jet. The symmetry of the profile meant that fluid must move across the center line to make up for the differing rates of entrainment. The best agreement with experimental was for the overall entrainment rate to be that of a free jet./3/

Regenscheit /4/, as well as the above authors, found that the reattachment length was independent of Reynolds number for fully turbulent jets. For this case, the reattachment point is therefore only dependent on geometry. Regenscheit gives equations for calculating the reattachment point to an offset flat plate parallel to the jet axis;

$$\frac{L}{w} = \left[0, 2 + 2, 7 \left(\frac{d}{w}\right)^{0, 8}\right] \tag{2.1}$$

and for a flat plate inclined to the axis of the jet;

$$\frac{L}{W} = \frac{4 \sin \alpha}{0.74 - 0.012 \,\alpha^{\circ}}$$
 (2.2)

Before reattachment, the jet is bounded by two curved shear layers. Curved shear layers were reviewed by Willie and Fernholz /5/. Castro and Bradshaw /6/ studied a highly curved mixing layer of a jet impinging normal to a flat plate. They provided information on turbulence characteristics and the effects of curvature on these. Gibson and Veriopoulos /7/ provided fluid mechanic as well as heat transfer data for a midly curved, heated boundary layer. They showed that even for mild curvature, there was significant effects on fluid dynamics as well as heat transfer.

Turbulent, reattaching flows have been more widely studied for backward facing steps or sudden enlargements in channels or pipes. Abbott and Kline /8/ studied the separated region for these geometries. They identified three zones of the separated region. A three dimensional zone immediately downstream of the step, a two dimensional zone downstream of the first and a time dependent tail region which changes in size in a periodic manner.

Eaton and Johnston /9/ reviewed literature for reattaching, turbulent flows. They found that there is a great effect on the reattachment length for flows of different states, laminar, transitional, or fully turbulent. Once the flows become fully turbulent however, the reattachment length becomes independent of Reynolds number. It was shown though that while the average reattachment point remains constant, it did fluctuate for a given flow, moving up and downstream.

Aung and Goldstein /10/ provided temperature profiles and heat transfer coefficients for a turbulent flow over a backward facing step using Mach-Zehnder interferometry. Their measurements showed general characteristics of the flow. The largest temperature gradients are located in the shear layer before reattachment with almost no temperature gradient across the separated region. The heat transfer coefficients were initially below the values for a flat plate in the separated region, rising to a peak value above that for a flat plate at or near the reattachment point. Downstream, the values relaxed to those of a flat plate.

Vogel and Eaton /11/ made detailed measurements of fluid dynamics and heat transfer for the same geometry. They showed that the Stanton Number peaked just up stream of reattachment. This peak was on the order of 0.1 step heights upstream of the reattachment point.

Seki et al /12/ studied a double step geometry. They also found similar temperature and velocity profiles in the areas

of separation. While the reattachment lengths differed, a similar peak in heat transfer was observed near the point of reattachment.

The above studies were done for low speed, turbulent flows. Data exists also for high speed separated flows, Lamb /13/, as well as for the laminar case, Aung /14/.

Gooray et al /15/ used a modified version of the $k-\epsilon$ turbulence model to make predictions of the heat transfer associated with rearward facing steps as well as sudden pipe expansions. Their computed values show good agreement with the studies mentioned above.

Bourque /1/ showed that at some point after reattachment, the separated, turbulent, plane jet takes on the characteristics of a plane, turbulent wall jet. Wall jets have been widely documented. Glauert /16/ and Schwarz and Cosart /17/ showed that isothermal wall jets take on a universal velocity profile when non-dimensionalized in the appropriate manner. Faeth and Liburdy /18/ showed that, for a weakly buoyant, turbulent wall flow, temperature profiles can also be presented in a universal profile.

COMPUTER PROGRAM

The computer model used for comparison with the experimental is based on work done by Spalding and Pun /20/. The program solves a set of two dimensional, elliptic equations for the $k-\varepsilon$ turbulence model using a finite difference method. Details of the fundamental equations and the numerical method used are described by Patankar /21/.

The model was adapted by Schmitz /19/ for the application of predicting the air movements in an indoor swimming pool. The $k-\varepsilon$ model was modified to include effects of buoyancy and wall damping of turbulence.

The equations solved by the program include continuity;

$$\frac{\partial}{\partial x}(\rho u) + \frac{\partial}{\partial y}(\rho v) = 0$$

momentum in the x direction;

$$\frac{\partial}{\partial x}(\rho u^{2}) + \frac{\partial}{\partial y}(\rho uv) - \frac{\partial}{\partial x}(\eta_{eff} \frac{\partial u}{\partial x}) - \frac{\partial}{\partial y}(\eta_{eff} \frac{\partial u}{\partial y})$$

$$= -\frac{\partial}{\partial x}(p + \frac{2}{3}\rho k) + \frac{\partial}{\partial x}(\eta_{eff} \frac{\partial u}{\partial x}) + \frac{\partial}{\partial y}(\eta_{eff} \frac{\partial v}{\partial x})$$

momentum in the y direction;

$$\frac{\partial}{\partial x}(\rho u v) + \frac{\partial}{\partial y}(\rho v^{2}) - \frac{\partial}{\partial x}(\eta_{eff} \frac{\partial v}{\partial x}) - \frac{\partial}{\partial y}(\eta_{eff} \frac{\partial v}{\partial y})$$

$$= -\frac{\partial}{\partial v}(p + \frac{2}{3}\rho k) + \frac{\partial}{\partial x}(\eta_{eff} \frac{\partial u}{\partial y}) + \frac{\partial}{\partial y}(\eta_{eff} \frac{\partial v}{\partial y}) - \rho g$$

energy;

$$\begin{split} &\frac{\partial}{\partial x}(\rho u h_{t}) + \frac{\partial}{\partial y}(\rho v h_{t}) - \frac{\partial}{\partial x}(\frac{\eta_{eff}}{Pr_{eff}} \frac{\partial h_{t}}{\partial x}) - \frac{\partial}{\partial y}(\frac{\eta_{eff}}{Pr_{eff}} \frac{\partial h_{t}}{\partial y}) \\ &= -\frac{\partial}{\partial x} \left[\frac{\eta_{eff}}{Pr_{eff}}((1 - \frac{Pr_{eff}}{Sc_{eff}}) (h_{D} - h_{L}) \frac{\partial \xi_{D}}{\partial x}) \right] \\ &- \frac{\partial}{\partial y} \left[\frac{\eta_{eff}}{Pr_{eff}}((1 - \frac{Pr_{eff}}{Sc_{eff}}) (h_{D} - h_{L}) \frac{\partial \xi_{D}}{\partial y}) \right] \end{split}$$

and water vapor concentration;

$$\frac{\partial}{\partial \mathbf{x}}(\rho \mathbf{u} \xi_{\mathbf{D}}) + \frac{\partial}{\partial \mathbf{y}}(\rho \mathbf{v} \xi_{\mathbf{D}}) - \frac{\partial}{\partial \mathbf{x}}(\frac{\eta_{\mathbf{eff}}}{Sc_{\mathbf{eff}}} \frac{\partial \xi_{\mathbf{D}}}{\partial \mathbf{x}}) - \frac{\partial}{\partial \mathbf{y}}(\frac{\eta_{\mathbf{eff}}}{Sc_{\mathbf{eff}}} \frac{\partial \xi_{\mathbf{D}}}{\partial \mathbf{y}}) = 0$$

The equation for the kinetic energy is;

$$\frac{\partial}{\partial x} (\rho u k) + \frac{\partial}{\partial y} (\rho v k) - \frac{\partial}{\partial x} (\frac{\eta_{eff}}{\sigma_{k,eff}} \frac{\partial k}{\partial x}) - \frac{\partial}{\partial y} (\frac{\eta_{eff}}{\sigma_{k,eff}} \frac{\partial k}{\partial y}) = \rho (P + G - \epsilon)$$

while the dissipation is described by;

$$\frac{\partial}{\partial x} (\rho u \varepsilon) + \frac{\partial}{\partial y} (\rho v \varepsilon) - \frac{\partial}{\partial x} (\frac{\eta_{eff}}{\sigma_{\varepsilon,eff}} \frac{\partial \varepsilon}{\partial x}) - \frac{\partial}{\partial y} (\frac{\eta_{eff}}{\sigma_{\varepsilon,eff}} \frac{\partial \varepsilon}{\partial y}) = \rho \frac{\varepsilon}{k} (C_1 P - C_2 \varepsilon)$$

The production of kinetic energy, P, is given by;

$$P = \frac{\eta_t}{\rho} \left[2 \left(\left(\frac{\partial u}{\partial x} \right)^2 + \left(\frac{\partial v}{\partial y} \right)^2 \right) + \left(\frac{\partial u}{\partial y} + \frac{\partial v}{\partial x} \right)^2 \right]$$

The G term models production of kinetic energy by buoyancy with;

$$G = \frac{a}{a^2} \frac{a^2}{a^2} \frac{a^3}{a^4}$$

The coefficients are given by;

$$\eta_{\text{eff}} = \eta + \eta_{\text{t}}$$
 and $\frac{\eta_{\text{eff}}}{Pr_{\text{eff}}} = \frac{\eta}{Pr} + \frac{\eta_{\text{t}}}{Pr_{\text{t}}}$

with the other coefficients broken into similar components. The turbulent Prandtl and Schmidt numbers are described by;

$$Pr_t$$
, $Sc_t = f(Distance from the wall, Buoyancy)$

The turbulent viscocity is;

$$\eta_{t} = c_{\eta} \cdot \rho \cdot \frac{k^{2}}{\epsilon}$$

where;

$$C_{\eta} = f(Distance from wall, Buoyancy)$$

The constants used are;

 ${\tt c}_{\tt 1} \qquad {\tt c}_{\tt 2} \qquad {\tt \sigma}_{\tt k} \qquad {\tt \sigma}_{\tt \epsilon}$

1,43 1,92 1,0 1,3

4. EQUIPMENT AND PROCEDURE

The measurements of the jet were done in a climate controlled room designed to simulate the air movements in indoor swimming pool. One wall is made of copper and can be heated or cooled to simulate a window exposed to environment. The jet inlet is located at the base of this jet temperature and flow rate can copper wall. The A pool is located at the center of the room which can also be heated to a desired temperature. The walls the room are insulated to insure two dimensional behavior.

Figure 1 shows the general flow patterns of the room and air conditioning equipment. The entire system is divided into two sections. The first section includes the measuring room and its air conditioning system. The second section includes a second chamber and its air conditioning system. The two sections are divided by a wall made of copper to provide good heat transfer between the two sections.

Air enters the measuring chamber at the base of this copper wall. The exit is located at the top of the other end of the After leaving the room, the air passes through a room. of conditioning systems. The first is a dehumidifiers. The dry air is then passed to a heaters which are used to establish the desired inlet temperature. The inlet temperature is measured using a type k thermocouple located at the inlet to the room. Flow rate is monitored by measuring the pressure drop across and orifice located between the two mixing chambers. passing through the second mixing chamber, the conditioned air reenters the measurement room.

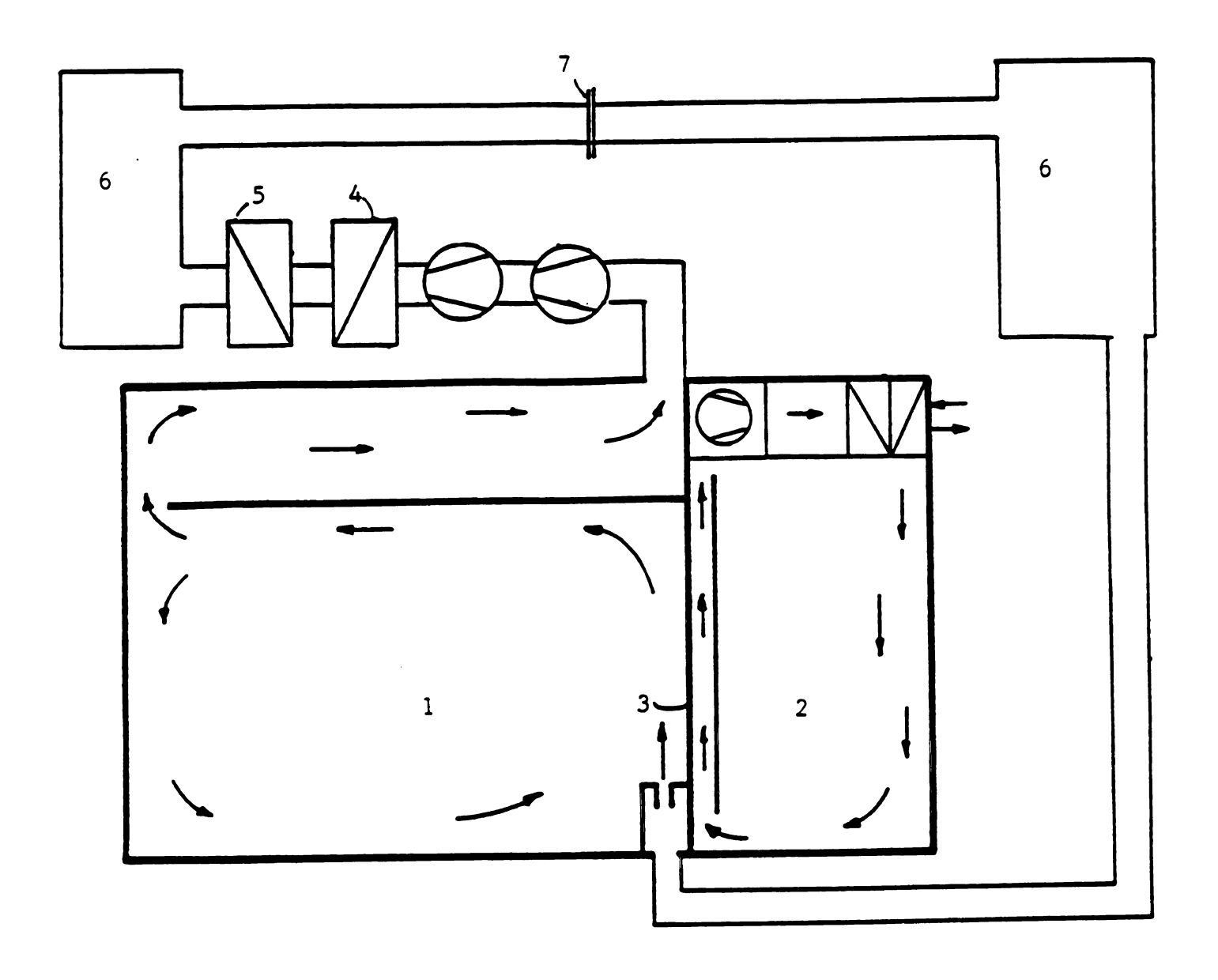


Figure 1 Climate Control System

- (1) Measurement Chamber
- (2) Cooling Chamber
- (3) Copper Wall
- (4) Dehumidifiers
- (5) Heaters
- (6) Mixing Chambers
- (7) Pressure Orifice

purpose of the second chamber is to simulate a desired environment condition on the copper wall. This is done by controlling the temperature on this side of the wall. As can be seen, the air flows parallel to the jet on the other side of the wall. The air passes through the conditioning system. which can either heat or cool the air. and reenters the chamber from the top. This system does not allow for a wall temperature to be selected. but rather the temperature of the air on this side of the copper wall. For the present study, two conditions are primarily used, the only exception described in a later section (5.2.4 CHANGE TEMPERATURE). The first condition is with the air set at a temperature of 10°C. This is designated as the "on" condi-The "off" condition is where the air conditioning tion. system was turned off and the air temperature in the chamber was dictated by the measurement room temperature.

inlet of the jet to the room is pictured in figure The air from the conditioning system flows into the inlet from one side of the room. It enters a channel located below set of honeycombs. which act as flow straighteners. To insure that the same flow rate exits across the therefore two dimensionality is achieved, plates are used to cover a portion of the honeycomb. The area throughwhich the air is allowed to pass is tapered and decreases across the Two right angle aluminum brackets are used to form inlet. the nozzle of the jet. These can be placed at varying distances from each other and from the copper wall to create different slot widths, w, and step heights, d, Slot widths of 5,10 and 20 millimeters were used along with step heights of 100 and 175 millimeters to achieve the ratios of d/w discussed later. These brackets were replaced by steel brackets at a 15° angle to the wall for the case of the jet issuing at an angle. the slot width was 10mm and the inlet to the room was located 100 mm from the copper wall.

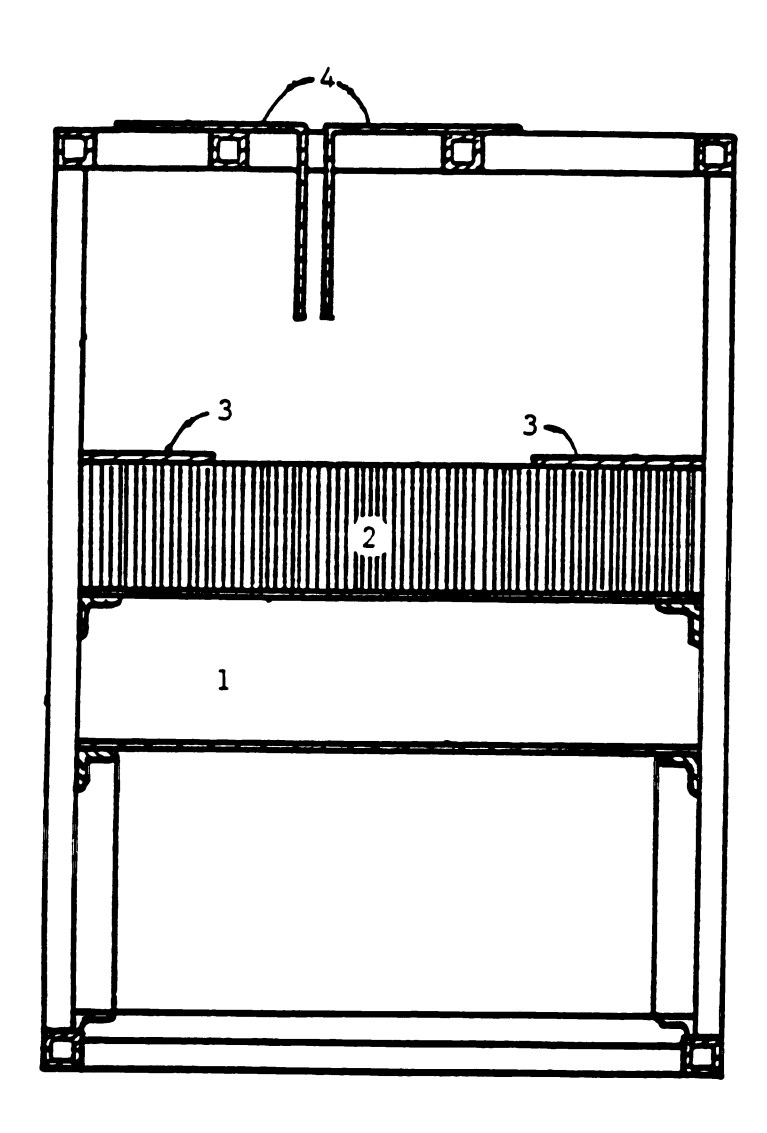


Figure 2 Inlet Structure; (1) inlet channel, (2) honeycomb (3) narrowing plates, (4) movable brackets

The reattachment lengths of the jet were found using a series of tissue paper flags attached to the copper wall with hinge lines perpendicular to the mean flow direction. as two dimensional tufts to indicate the acted flow direction.(fig. 3) This technique is similar to that used by Bourque /2/. The separation length was defined as the furthest downstream to indicate a recirculating This was found by observing the flags through a window from outside the measurement room. When this fluctuated, the range of fluctuation was noted and the median value taken to be the nominal reattachment length. staggered, parallel rows of flags were used. The spacing between each row was two centimeters, resulting in an overall accuracy of within one centimeter. Figures 4 and 5 show the relative placement of these flags with respect to the other equipment.

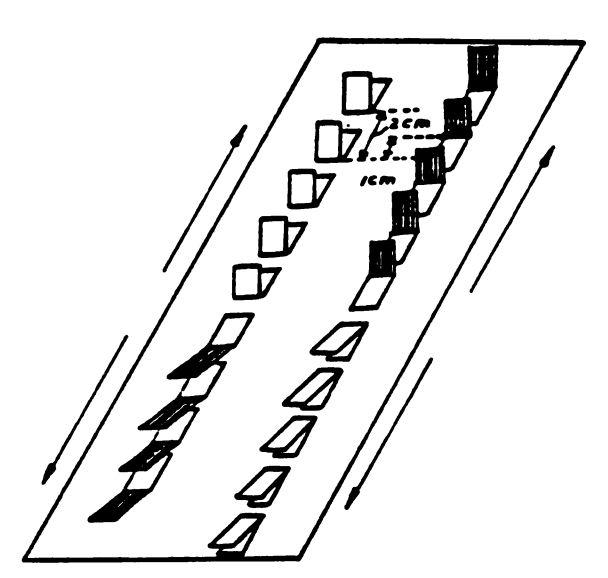
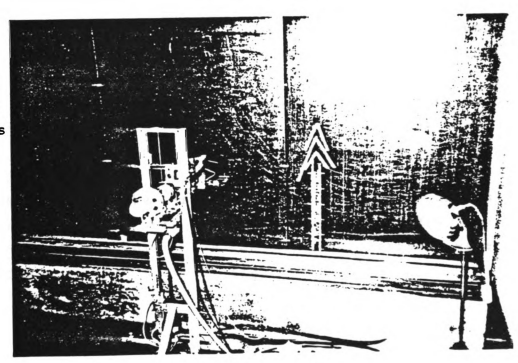


Figure 3 Reattachment Indicators

Figure 4 Reattachment Flags



Figure 5
Robot and
Reattachment Flags



The other measurements were done with two sets of equipment, one for the reattaching region and one for the wall jet or developed region downstream. In the region close to the jet inlet, velocity measurements were done using a DISA 55P81 temperature compensated hotwire with a standard bridge. Temperature measurements were performed with a type T thermocouple. The concentration of water vapor was found with a model DP4-D dew point mirror by MBW Electronics, Switz.. A robot was used to position the probes to the appropriate measuring locations. (fig. 6)

A different robot was used in the region farther downstream in the developed region. This was the robot used for the room air measurements.(fig. 7) The velocity in this region was determined using a TSI model 1610 velocity transducer, a hot film anamometer.

All data gathering in both regions was done by an Orion Data Logger 3530 A by Schlumberger Electronics Ltd.. At each measuring point, 200 data points were gathered at 5 Hz and were statistically analyzed. The averages and standard deviations were output to an Apple IIe computer which cataloged and stored the data. For a more detailed account of the data reduction routines, the reader is referred to the work of Ewes (25).

Measurements of the reattaching region as well as the developed region were done at the centerline of the room. (Fig. 8) The reattachment lengths were measured away from the centerline so that there was no influence from the measuring equipment on the flags or vice versa. The checks for two dimensionality were done at 1/4, 1/2 and 3/4 the distance across the room. The reattachment lengths were checked at the positions shown on figure 8.

Figure 6 Measurement Robot for Grid

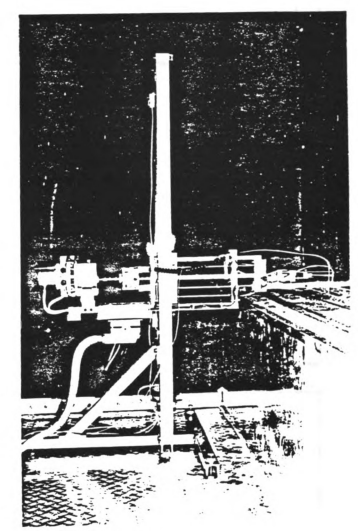
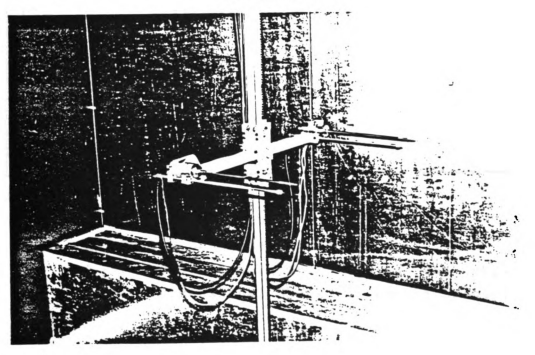


Figure 7 Room

Measuring
Robot



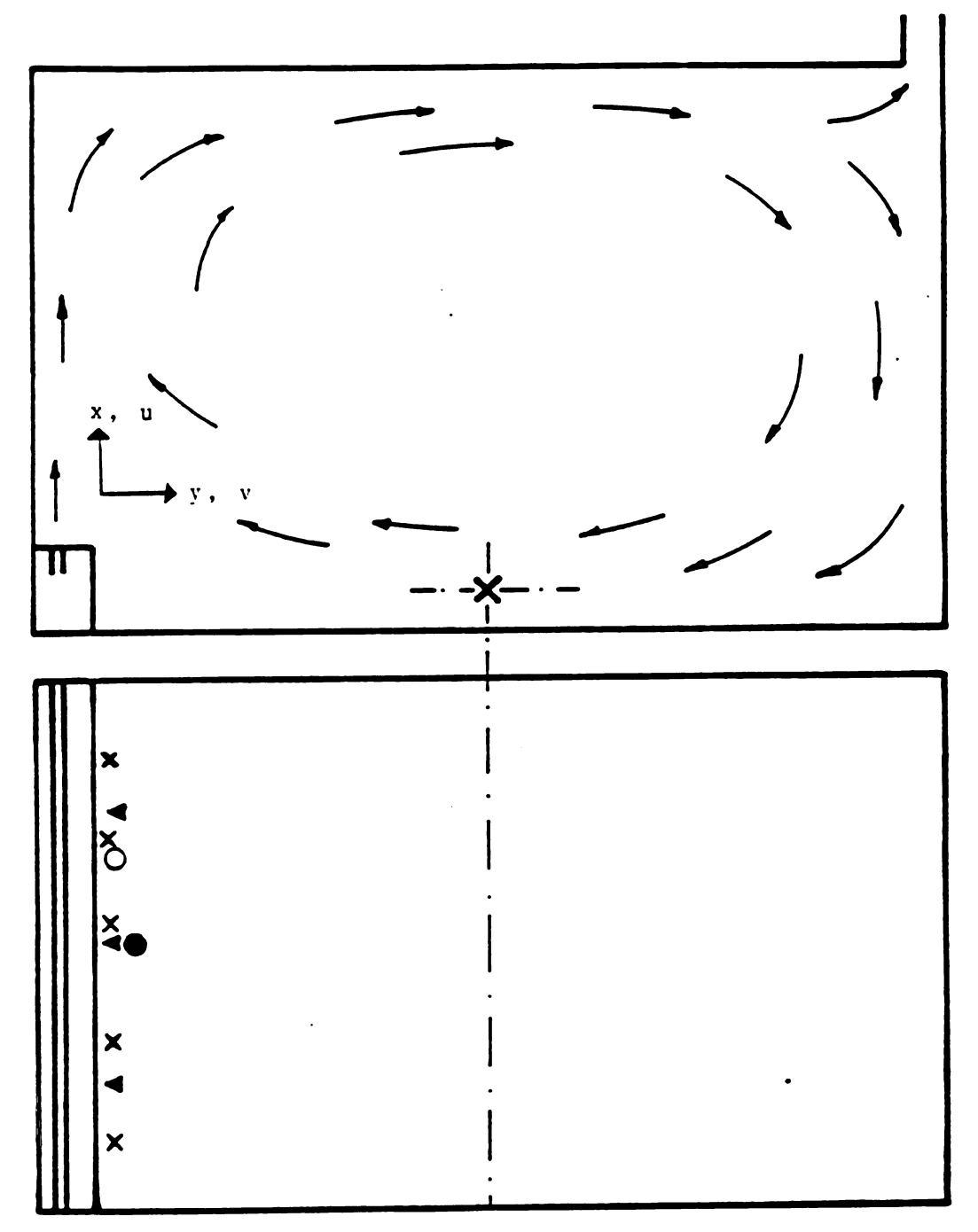


Figure 8 Measurement Positions

- - Grid Measurements
- O Reattachment Measurements
- ▲ Two-Dimensional Check for Vel. and Temp.
- $\dot{\chi}$ Two-Dimensional Check for Reattachment lengths

5. RESULTS AND DISCUSSION

The measurements performed can be divided into three groups. The first are a set of velocity and temperature profiles done different positions along the jet to document the dimensionality and the inlet conditions of the jet. second set are velocity, temperature, moisture concentration levels and reattachment lengths measured through grids for a number of different cases. (The different measurement grids used are pictured in Appendix A while a complete list of these measurements is located in B). The results are later compared with the computer program mentioned in the previous section. The last set measurements of velocity and temperature done along center of the room at higher positions than the grid to compare the later development of the jet with the computer predictions.

5.1 DOCUMENTATION OF THE JET

The inlet velocity profiles for all the parallel geometries studied are shown in figure 9. For the cases of d/w equal to 5, 10 and 17.5 a block profile is approximated. There is however a slight assymmetry in all these cases but is most prevalent for d/w=5. For the case of d/w=35 the profile has a developed, parabolic shape. The case of d/w=20 also shows signs of being developed but not nearly to the same extent.

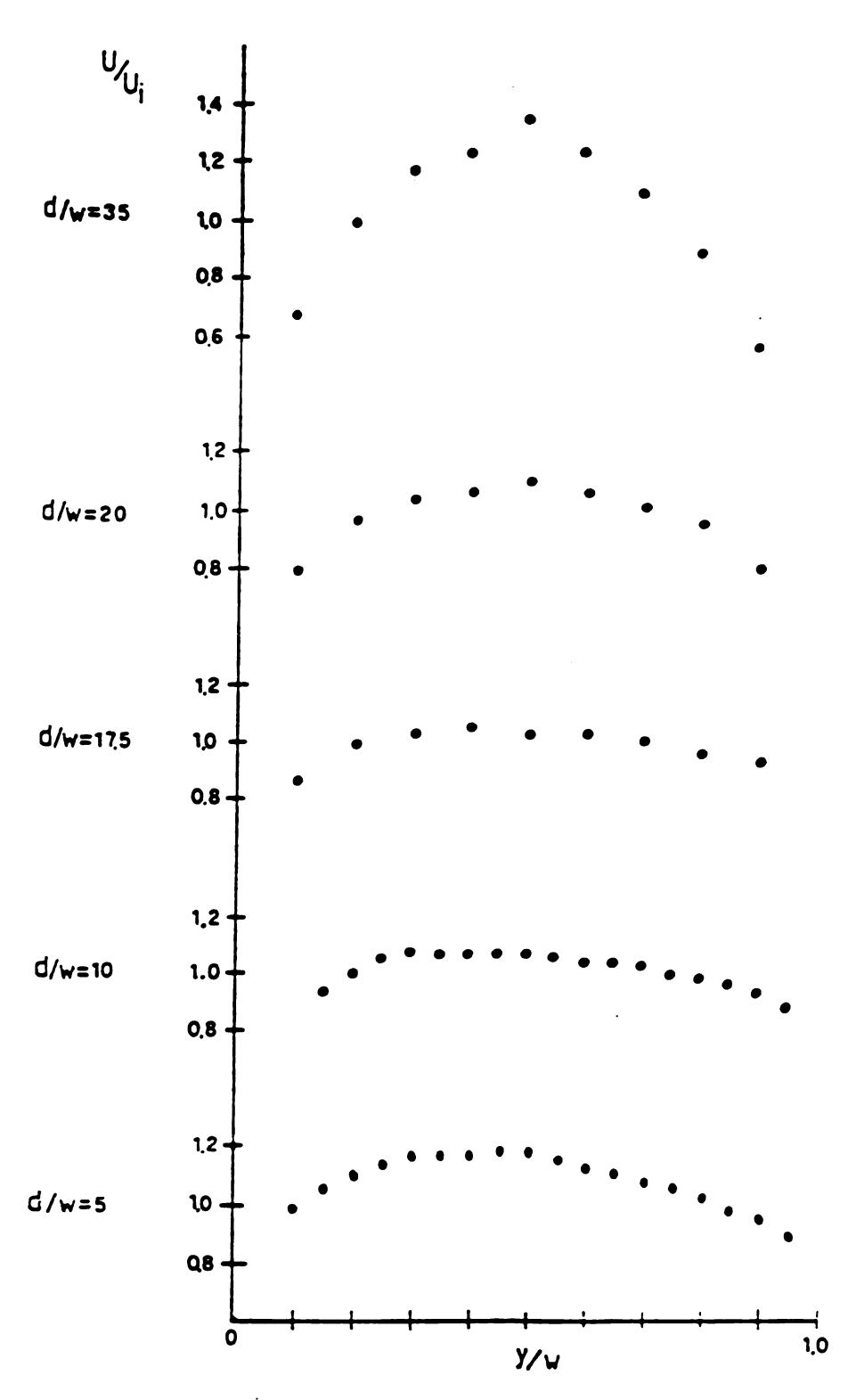


Figure 9 Inlet velocity profiles

For the cases of d/w=10 and Re=2500 and 3800, velocity, temperature and reattachment lengths were measured along the jet to insure two dimensionality. Velocity and temperature profiles were taken at the jet exit, 0.5L and 2L(figures 10-12). These show that the initial velocity is 5% higher in the center of the room than that closer to either side wall. This difference seems to disappear at 0.5L. At 2L, the center has a higher peak velocity, less than 5%, than the positions on either side. The temperature shows a gradient across the jet at the jet exit of order of 0.5 C. This gradient reduces to the order of 0.1 C for the higher profiles.

The reattachment lengths were measured along the wall. While there was some fluctuation at any given point (see later discussion of reattachment lengths) the distance remained constant to within the error of the measurement. (TABLE 1)

TABLE 1

POSITION	REATTACHMENT LENGTH (cm)
1	20
2	21
3	21
4	22
5	21

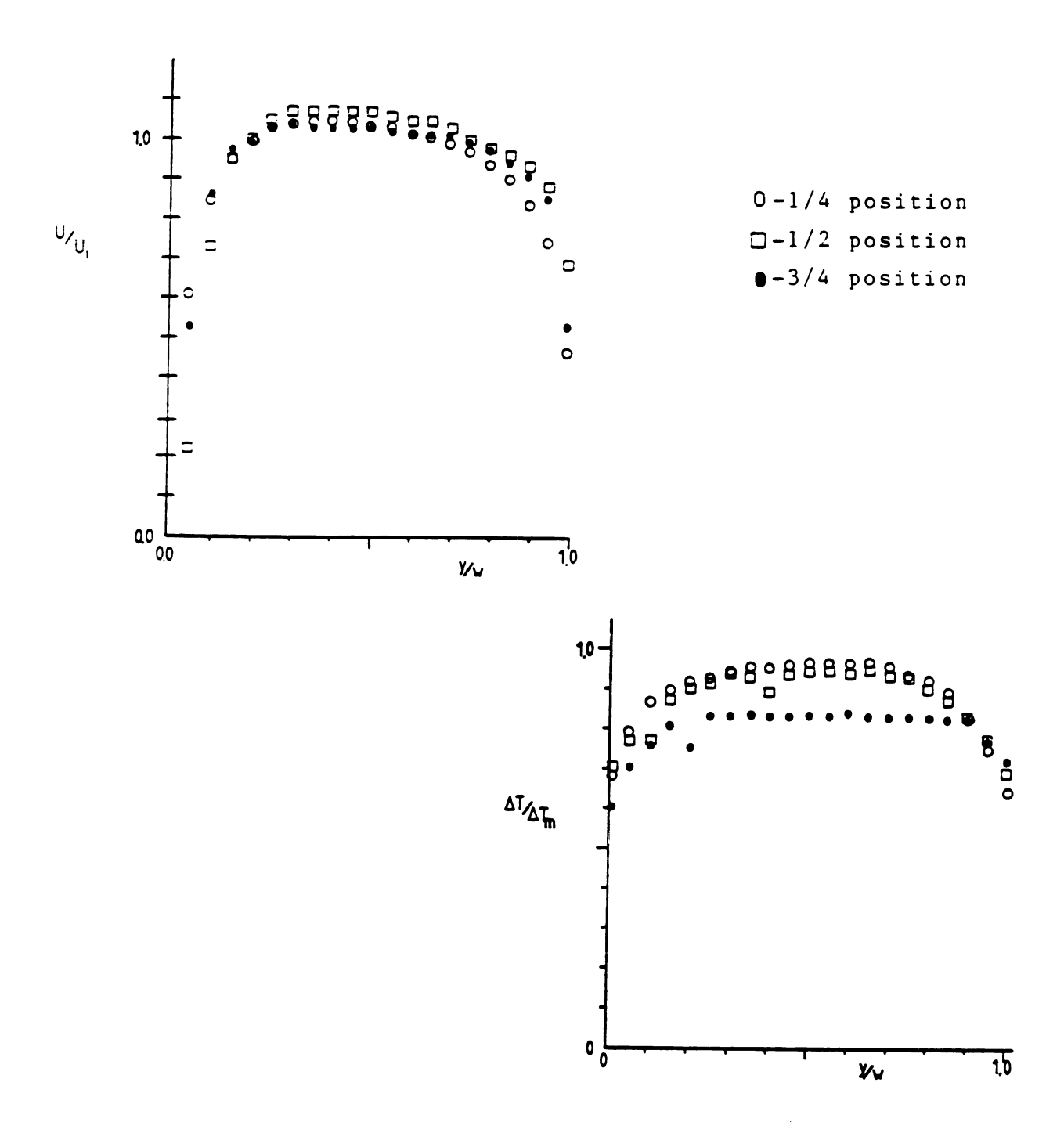
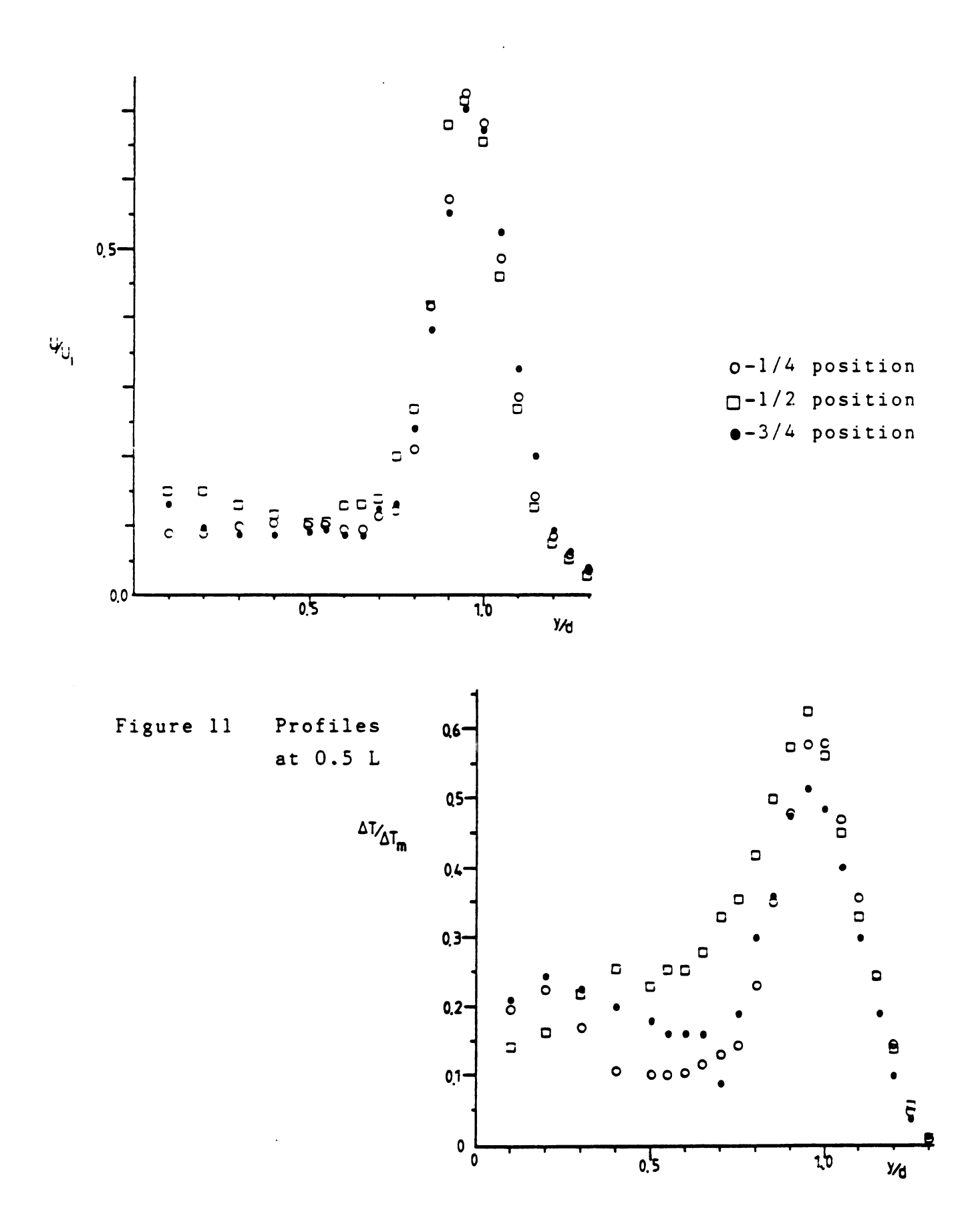


Figure 10 Profiles at jet inlet



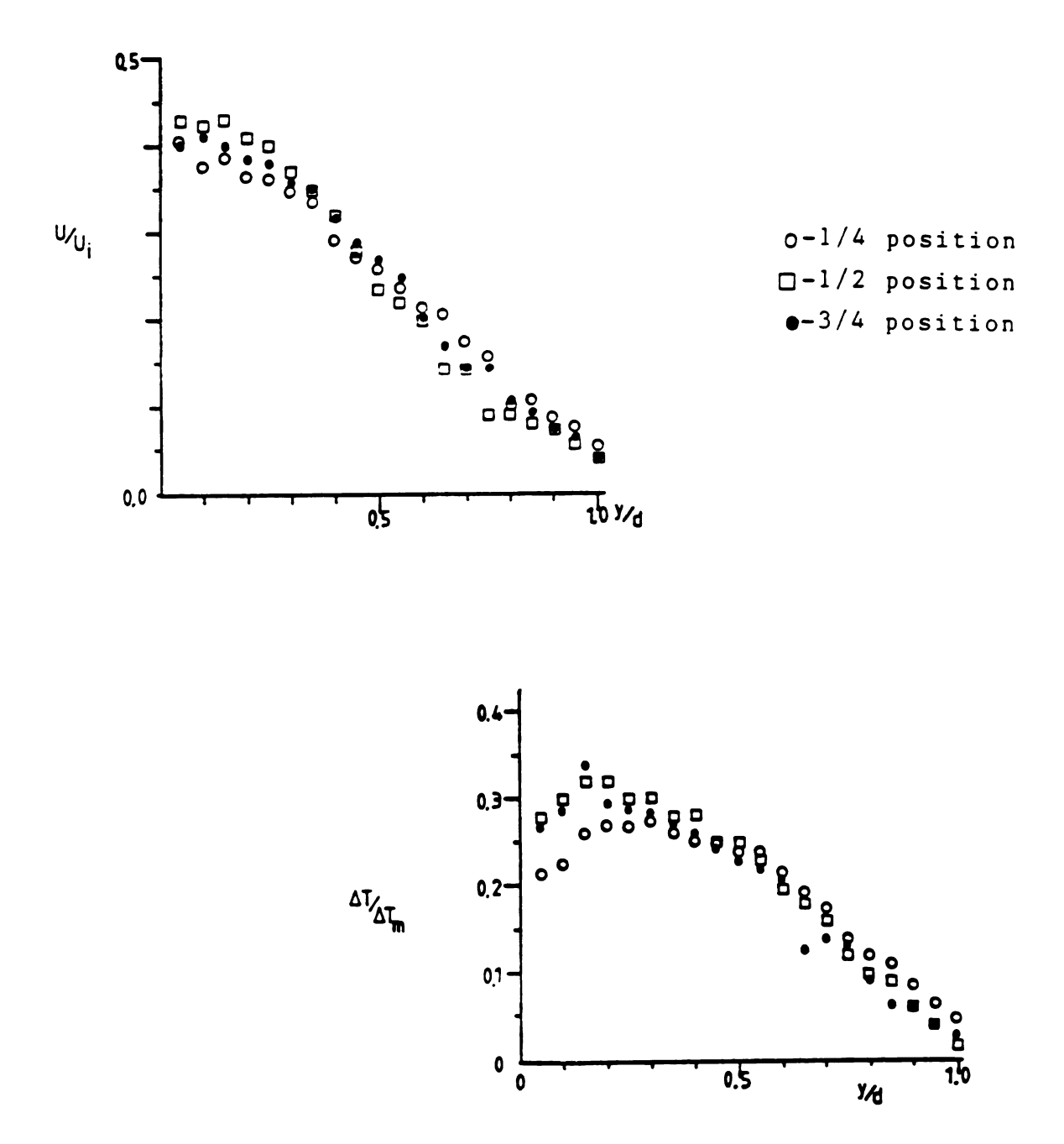


Figure 12 Profiles at 2L

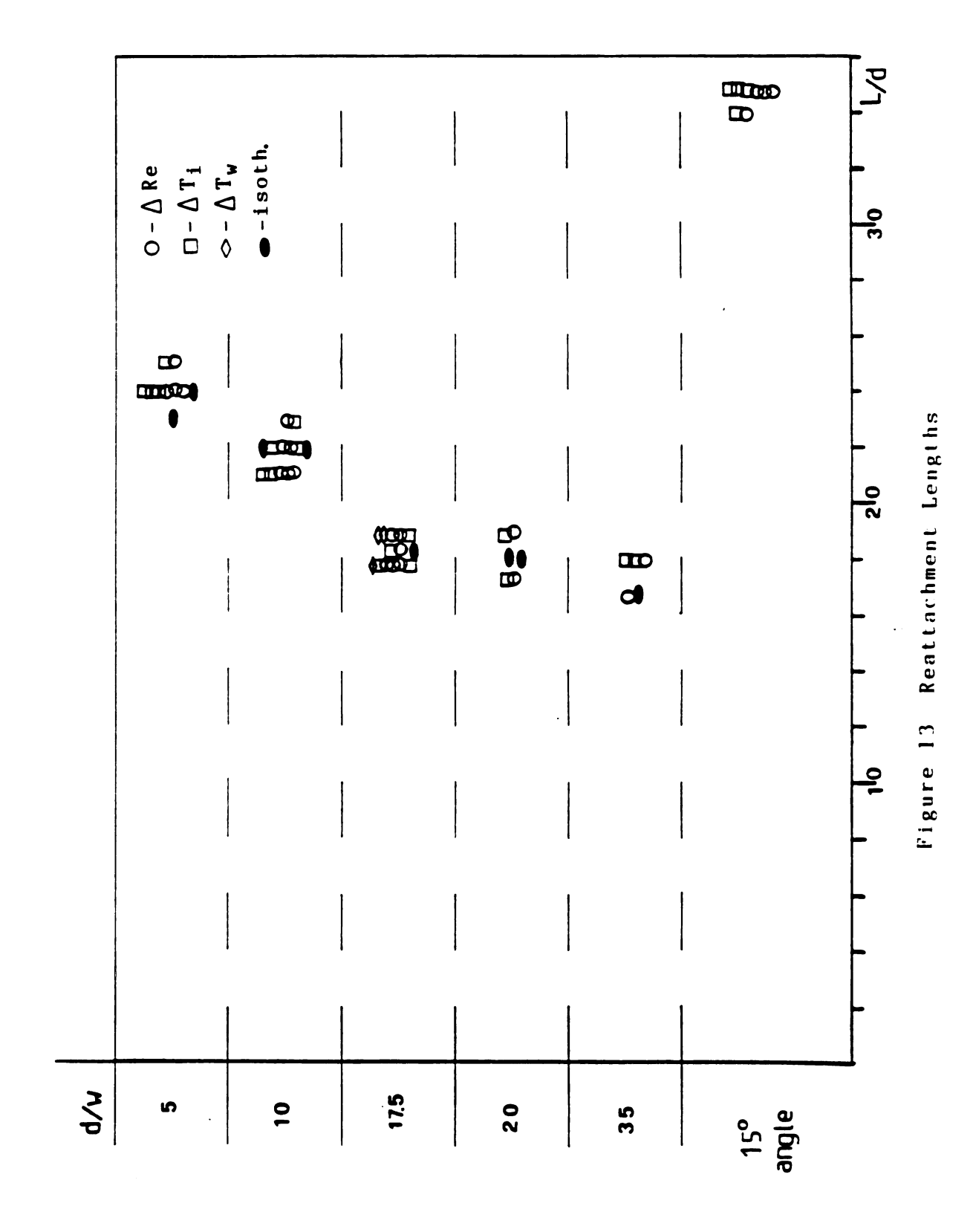
5.2 SEPARATED AND REATTACHING ZONE

The measurements discussed in this section are restricted to the measurement grids shown in appendix A. The results are divided into two parts. The first is a discussion of the reattachment distances and the effects of the system parameters used on them. The second is a discussion of the measurements done at the grid points. This second part will be subdivided by the parameters being discussed.

5.2.1 REATTACHMENT LENGTHS

Figure 13 shows the reattachment lengths for the cases studied. To within the accuracy of the measurements, there was no effect of inlet temperature, wall temperature or inlet velocity for any given geometry. While some slight deviations occured, there were no trends while parameters were varied. Since the isothermal cases showed the same reattachment lengths, the buoyancy forces do not appear to have an effect on them. The lack of changes with respect to changing Re indicates that all the cases are fully turbulent /4/.

For the cases where the flow rate at reattachment was the exact point was difficult to determine. This was especially true for the case of d/w=35. This may Another factor influencing scatter of some of the scatter. the data was the fluctuating of the reattachment point. has been observed by other authors /9/. The fluctuations that were observed were of the order of 0.1L. point was found by observation, there the possibility of some inaccuracty being introduced here. Ιf



	<u>.</u>
	?:

the fluctuation magnitudes are taken to be an error estimate, it can be seen that all the data for each geometry falls within these limits.

When the reattachment lengths for the parallel cases are compared with previous data (figure 14) it can be seen that the present data exhibits the same trend as the formula given by Regenscheit 4/4. The line connecting the present data has

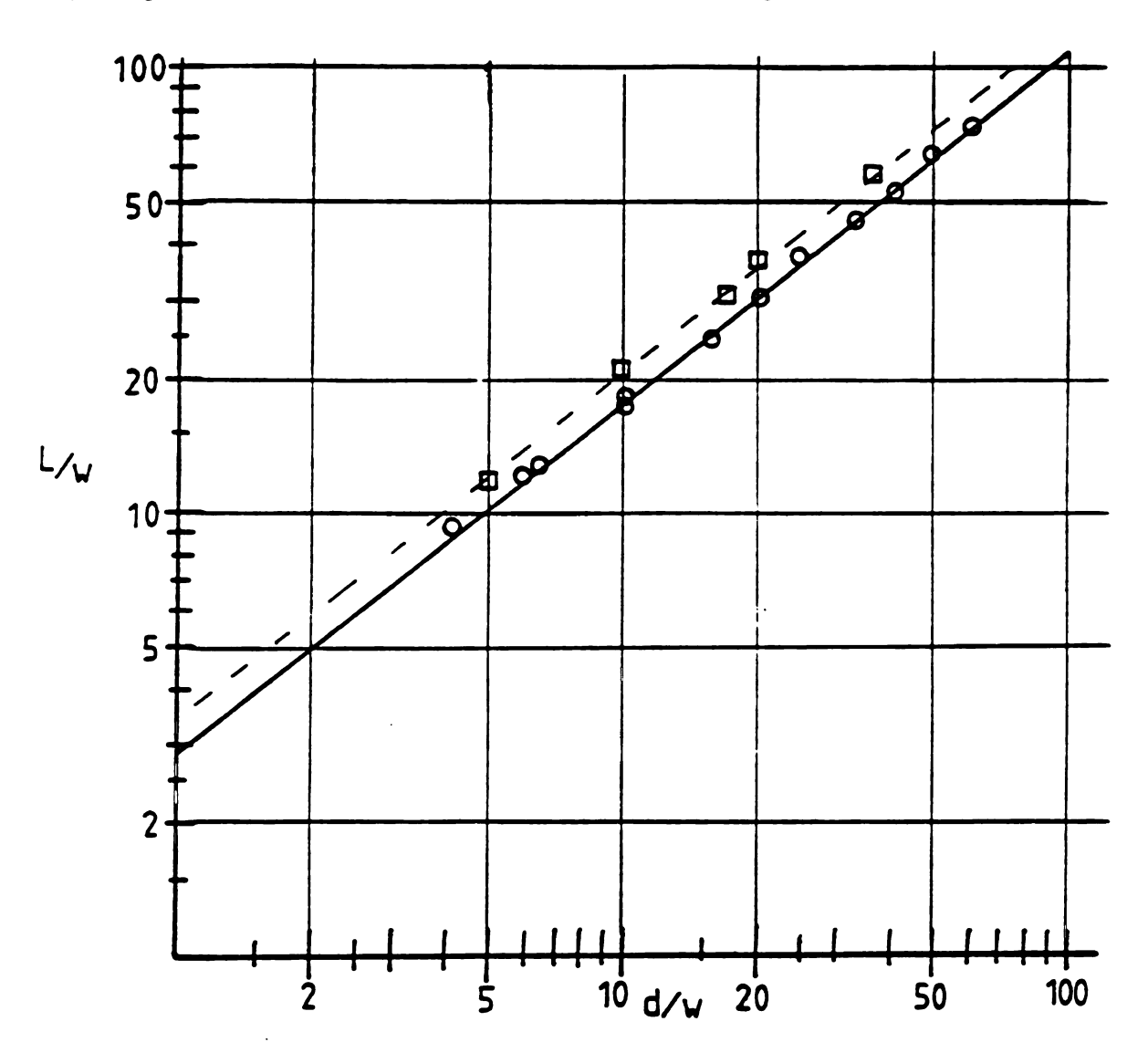
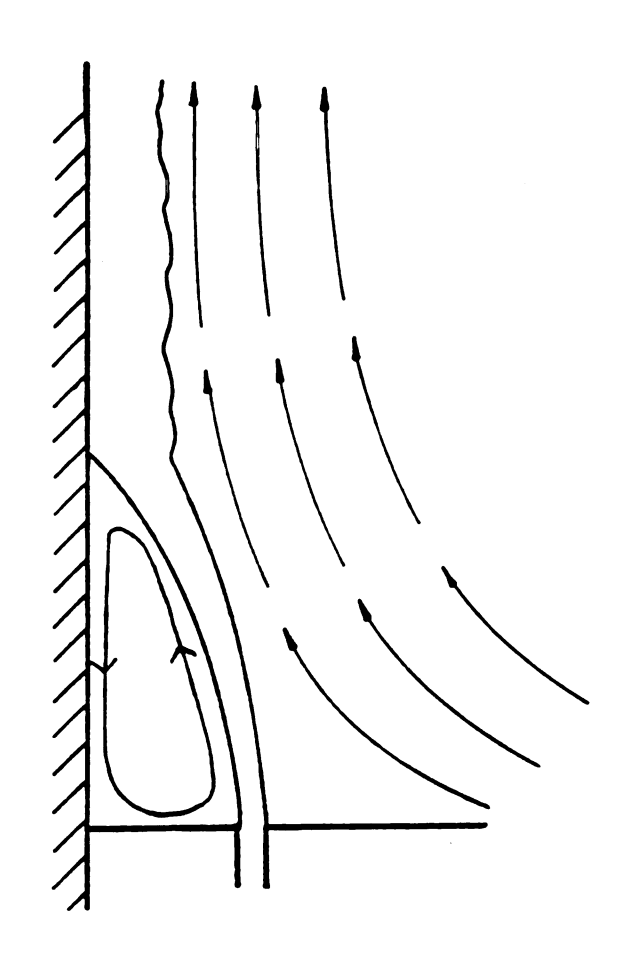


Figure 14 Reattachment lengths; O-previous data /4/

the same slope but it is clearly offset by a factor. This discrepancy can be explained by using the theoretical analysis of Sawyer /3/.

Sawyer's analysis allows the possibility for different rates of entrainment the two sides of the jet. His predictions are in good agreement with previous studies for the entrainment rates to be approximately the same for each side. These cases were done with an ambient velocity zero or close to zero. For this study, measurements were performed in the climate controlled room design to have air currents throughout the room. The jet under study therefore has a parallel current running along side it from the point it enters the room (fig. 15). Since this fluid is already

Figure 15 Parallel room currents to the jet



moving in the direction of the jet, less energy would be required to entrain the same amount of fluid. It seems reasonable that the jet would therefore entrain more fluid from the side exposed to the room. For the case of more entrainment on this side, Sawyer's analysis shows that the curves for reattachment move in the direction of the present data. While the exact ratio of entrainment is unknown, it seems possible that an appropriate curve could be drawn through the present set of data if it were known (fig 16).

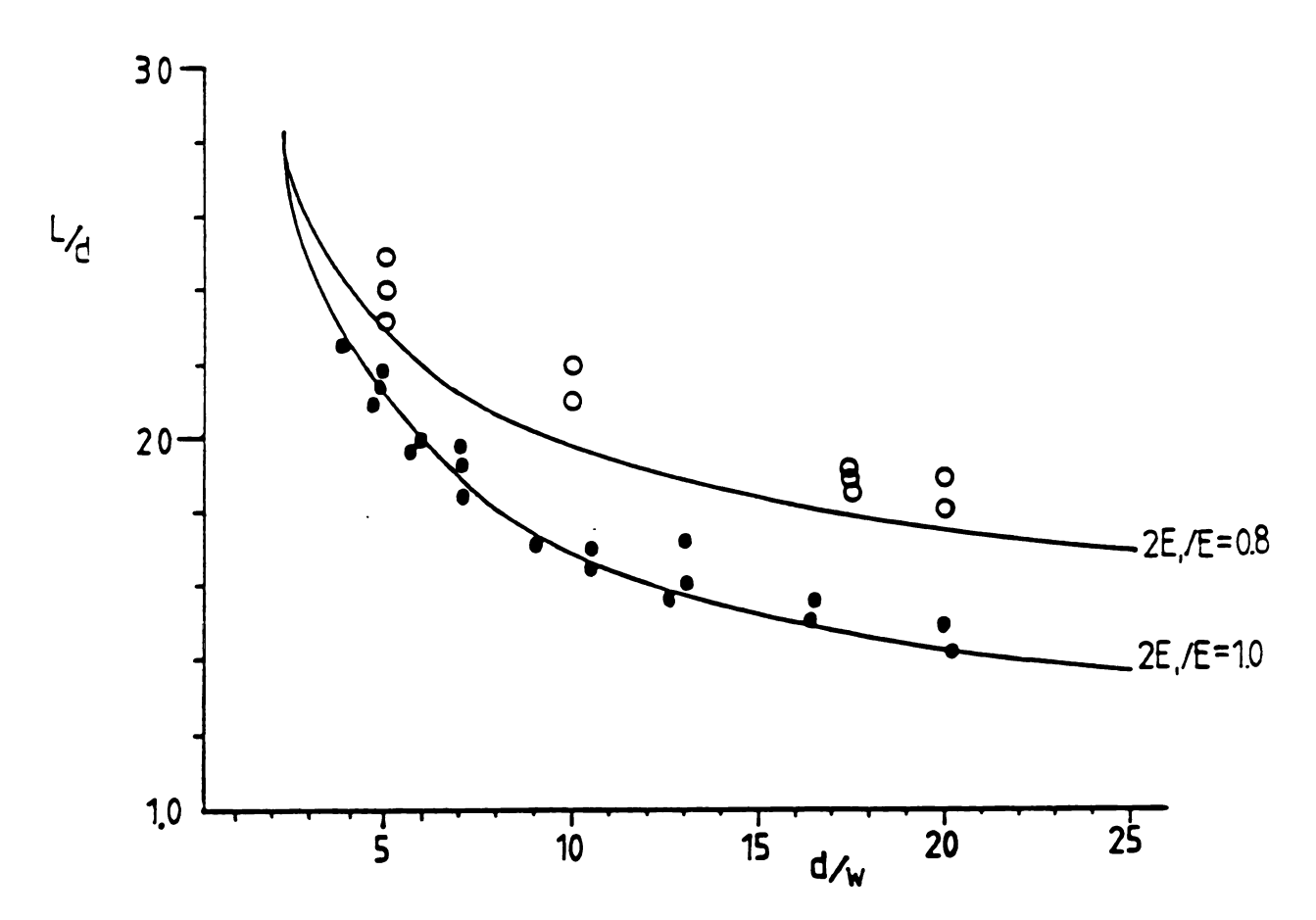


Figure 16 Analysis of Sawyer /3/ •-previous data o-present study

Physically this phenomenon seems reasonable. If more fluid was entrained by the jet, the pressure gradient across the jet would not be as great. Since it is the pressure gradient which overcomes the inertial forces and pulls the jet to the wall, this force would not be as great. The result is that the fluid would not be attracted to the wall as much and the distance which the jet takes to attach to the wall would be greater. The limiting case for this would be a channel flow over a backward facing step where the ambient and the jet were the same. For this case the separation lengths are indeed greater yet. Typical values are about 6d /10-12/.

Another possible factor exists to explain the dicrepancy between this study and previous data. The computer predictions (discussed in later section) show a region where the u components of velocity are negative, opposing the flow. (fig. 17) This appears for for the cases of d/w=5, 10, & 20

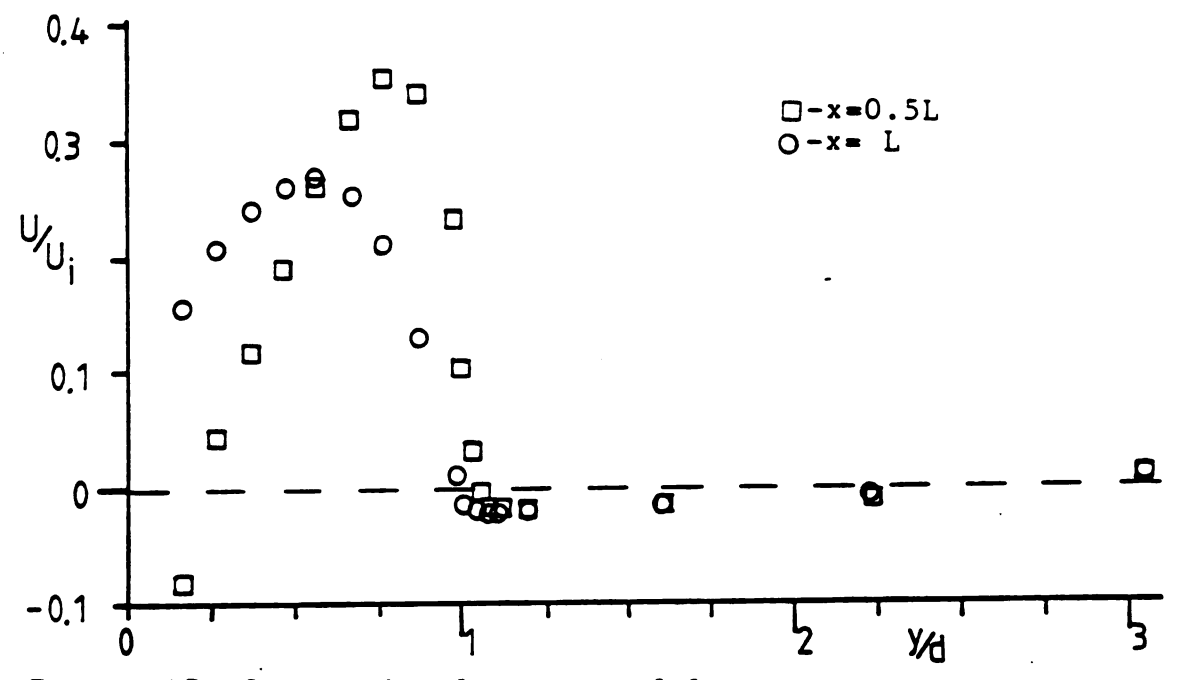


Figure 17 Computed velocity profiles

on the free side of the jet in the region before reattachment. This is due to the structure of the jet inlet obstructing the entraining fluid (figure 18). While this

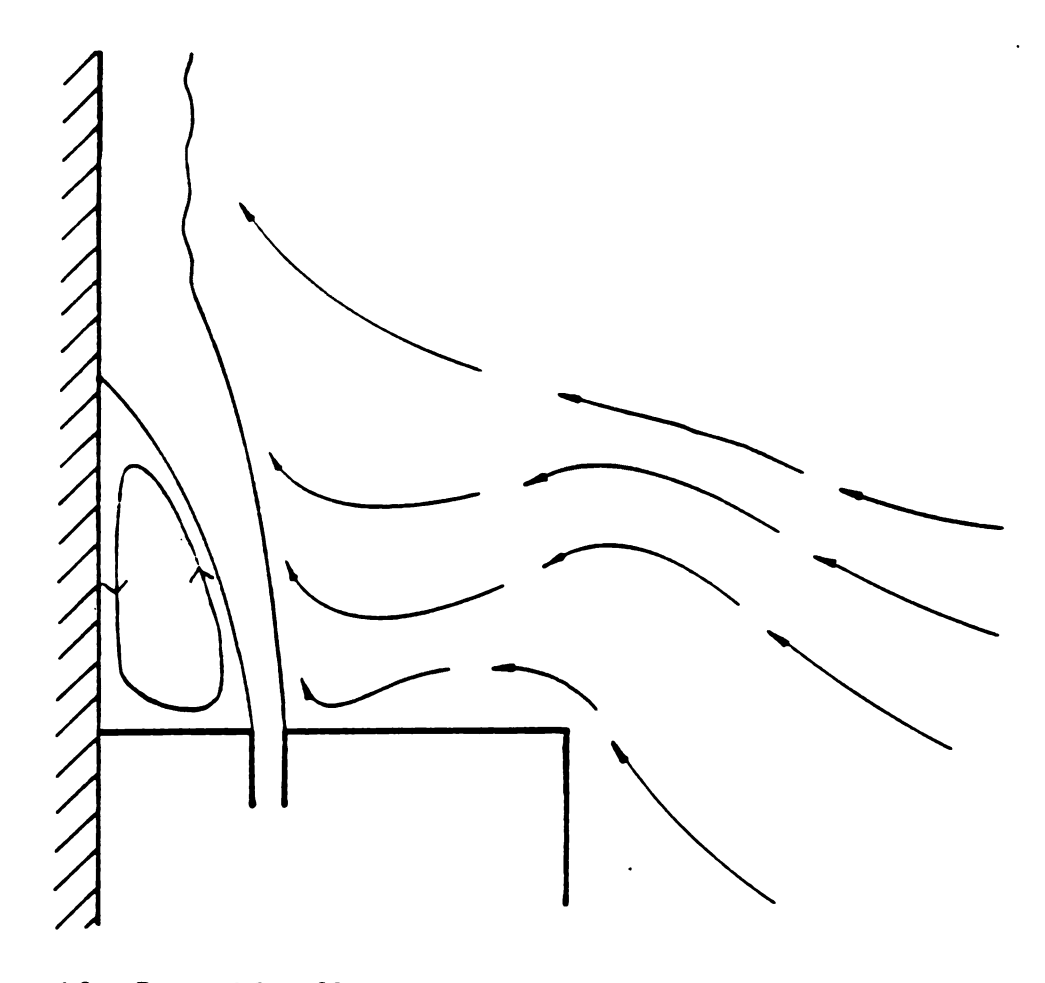


Figure 18 Possible flow patterns

seems to contradict the previous claim of enhanced entrainment, it produces the same result. The pressure in this zone would have to be subambient to change the direction of the streamlines. The pressure gradient across the jet would still be less than for the case of no ambient currents

as in previous studies. The result would therefore be the same, a greater reattachment length.

It is not clear which of these phenomenon is the actual cause for the discrepency. For the geometries of d/w=17.5and 35, where the jet issues closer to the edge of the inlet box, the program shows that the region of negative u velocity components does not extend for a significant part of the jet. If this is true for the measurement also, it means that this zone could not explain the discrepency in results for these is unclear if these zones even occur in the geometries. It flows since the measuring equipment used could experimental not distinguish the direction of velocities. A detailed study of this region would be required to answer It is clear though that the present affected in a systematic manner This effect is a result the ambient currents.

The last case for discussion is for the jet separated the wall and issuing at a 15° angle away from the wall. The separation distance is approximately twice that for the similar parallel geometry of d/w=10. Regenscheit /3/ poses formulas for the parallel case (2.1) and for a issuing at an angle (2.2) but not for the combined case. is clear that the two are not additive since the angle would only increase the separation length by 10% if this were true. This geometry would be influenced by the above effects of entrainment as the others. The effect may even be greater since the jet flows out into the mentioned currents. jet issues from the center of the inlet box where the reversing flow was observed for the computed, parallel cases similar situation may occur here as well. reattachment length is much greater, the effect of such a zone would be reduced. No literature for this geometry is available for comparison.

5.2.2 VELOCITY AND TEMPERATURE MEASUREMENTS

Velocity and temperature measurements are made for several different cases. The inlet conditions for Reynolds number and temperature are varied as well as the wall temperature. Geometry is also a variable in that the slot width, distance separating the wall from the jet and the angle of the jet were changed. The effects of these parameters are documented below.

For the velocity measurements, an isothermal case where buoyancy is not a factor is used for comparison. This was done by turning off the cold wall, or the air conditioning systems behind the wall, (see EQUIPMENT AND PROCEDURE), and setting the inlet temperature to 27° C. The pool was also set at 28° C, as it was for all cases. This produced a situation where the overall temperature gradient was of the order of 0.5° C or less.

It is difficult to isolate some of the parameters desired. A change in the one, say inlet temperature, changes the wall temperature as well as the ambient the jet sees. Table 2 provides the temperatures and the effects of each case under study. It is unclear which temperatures govern the characteristics of the flow. Because of this and because of the changing of the wall and ambient with measurement height, the cases are simply identified by the inlet velocity and temperature.

TABLE 2- Room and Wall Temperatures

d/w	Re	Ti	Wall Setting	Ta	T _w
		degC	deg. C	deg.C	deg.C
10	3600	38.7	10	29.0	20.0-25.0
10	3838	26.8	10	23.5	16.0-19.3
10	2071	27.1	10	22.5	15.0-17.5
10	1191	26.5	10	22.0	14.0-15.5
20	2022	27.4	10	22.5	15.5-17.8
10	3808	41.6	10	30.0	21.8-26.3
17.5	3800	37.9	10	29.8	18.3-24.0
17.5	2062	27.0	10	22.5	14.0-17.5
17.5	3755	27.2	10	24.3	15.5-19.5
17.5	3622	38.1	5	28.0	15.0-22.0
17.5	3688	38.6	off	32.5	32.5-33.5
10*	3824	27.3	10	23.5	16.0-19.0
5	· 7647	27.4	10	24.5	17.0-20.8

^{*-} jet issued at a 15° angle to the wall

The overall shapes of the velocity and temperature profiles are in general in good agreement with literature /10-12/. (figure 19) The shear layers of the velocity profiles locate the main temperature gradients. Almost no temperature gradients occur across the separated regions. The exception to this is discussed later (see CHANGE IN WALL TEMPERATURE). One feature which seems to disagree with previous studies is the uniformity of the velocity profile in the recirculation zone. The literature indicates that there should be a gradient across this zone with the sign of velocity changing. This phenomenon can not be observed using a hot wire probe since it does not distinguish directions. A minimum in the magnitude is expected however near the area of the change in

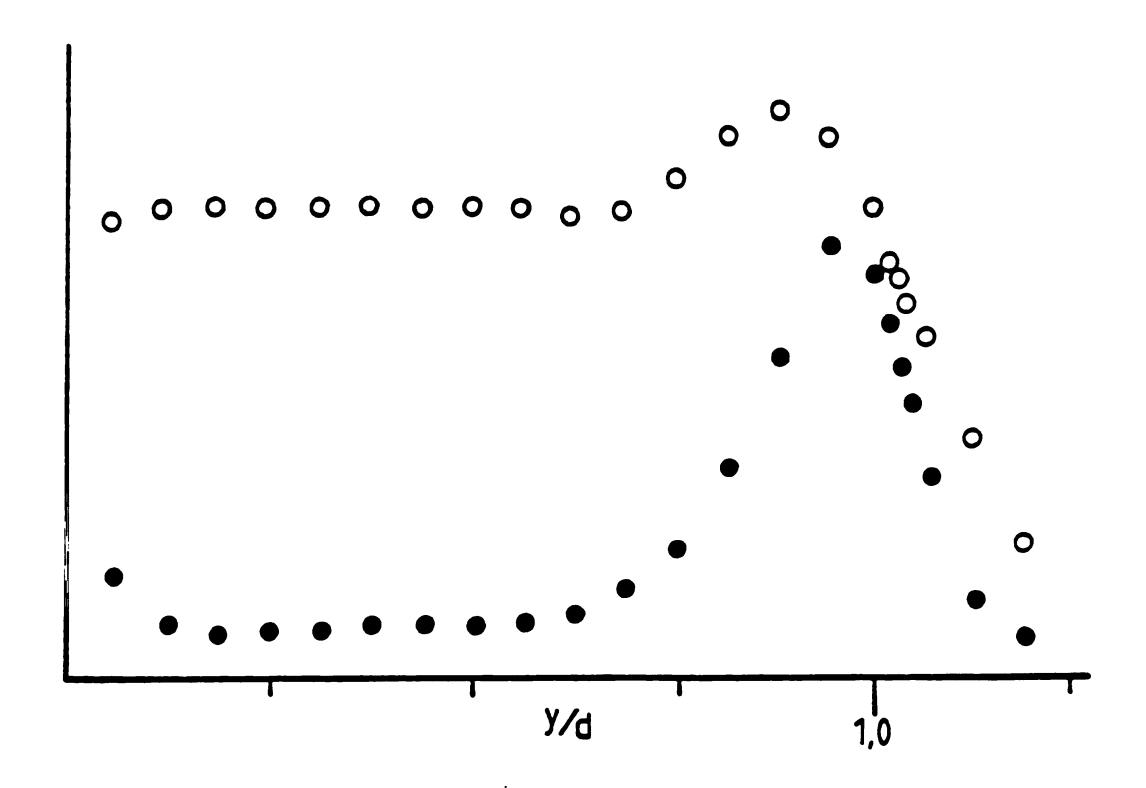


Figure 19 Velocity and Temperature Profiles •-velocity o-temperature

direction. The absence of such a minimum indicates that the flow must be very unsteady. This is in agreement with the previous observations of the fluctuations in reattachment points.

5.2.3 CHANGE IN INLET TEMPERATURE

For the study of the effect of inlet temperature on the jet, the geometry of d/w=10 and Re=3800 is used. Inlet temperatures of 27° C, 38° C and 42° C are used. The velocity profiles for the 38° case and the 27° case look very similar. (figure 20) Both show effects of buoyancy when compared to the isothermal velocity. The developed peak velocity is 15% higher than for the isothermal case. The case of 42° C shows a slightly different development. At the 3/4L position it can be seen that the jet seems to be moving toward the wall faster. There was no resulting effect on the reattachment length however (see previous section). The developed profile at the 2L position shows the same difference with respect to the other nonisothermal cases. The temperature profiles showed no other significant differences.

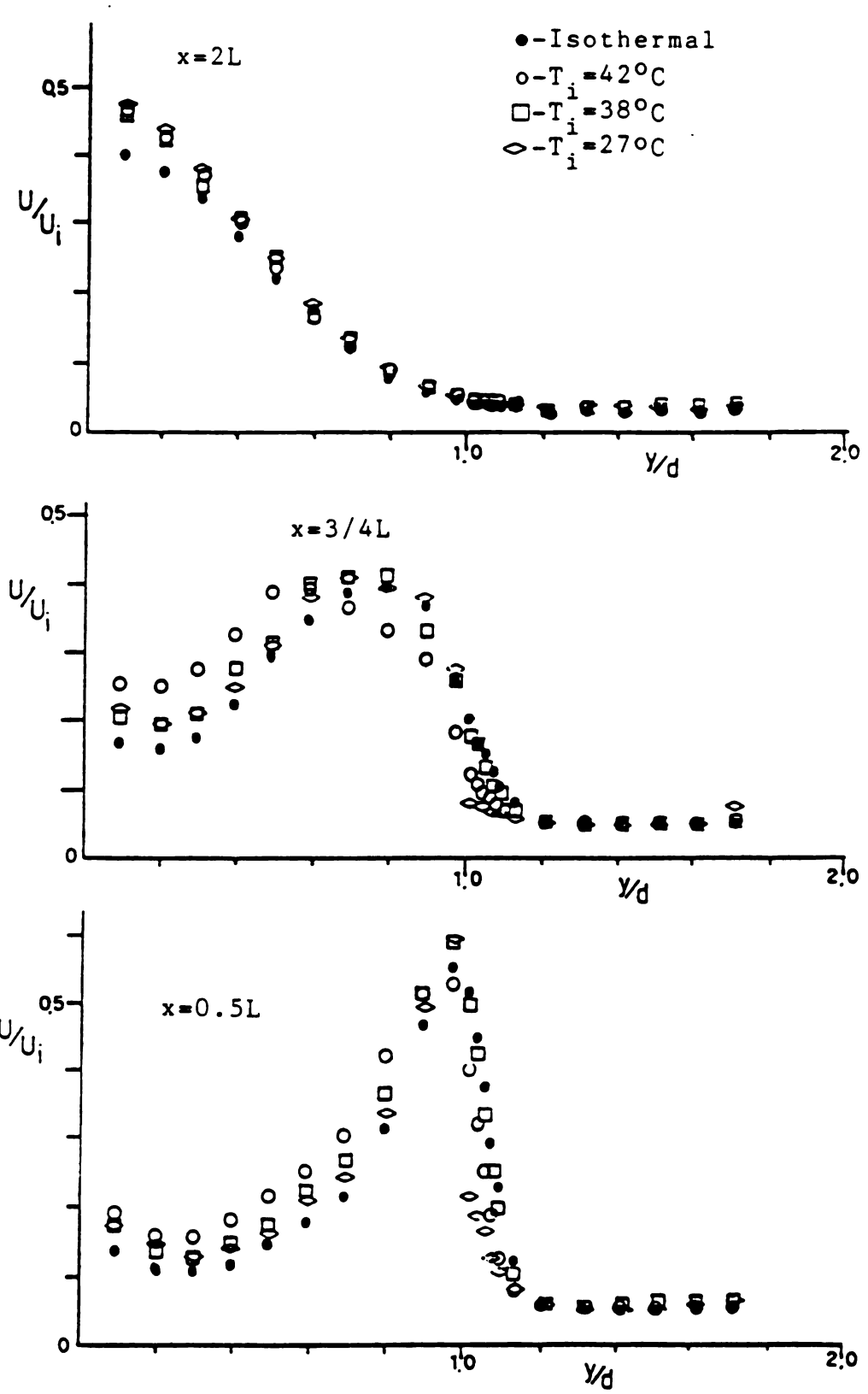


Figure 20 Velocity Profiles for Changes in Inlet Temperature

5.2.4 CHANGE IN WALL TEMPERATURE

The setting for the wall temperature could be changed. While the exact temperature of the wall could not be set, the temperature of the air on the cooling side could be set (see Equipment and Procedure section). Three different settings were used. The wall was set for 5° C, 10° C and turned off. Each of these cases effected the ambient temperature also (see Table 2). For all three cases, a Re=3800, d/w=17.5 and an inlet temperature of 38° C was used.

These changes produced little change in the velocity profiles(figure 21). In the case where the wall was off, the profiles seem to be moving closer to the wall. This would indicate that it is developing into a wall jet faster. Unfortunately, the measurement grid does not allow further positions to be measured so that the developed region can not be compared.

The temperature profiles show a definite difference in separated region. The difference occurs between the cases of the wall on and off (figure 22). When the wall is on, there is a significant minimum in the middle of the separated This violates previous studies /10/ as well as the laws of thermodynamics since the colder fluid is by warm fluid in a steady state condition. explained by the test equipment itself. For the cases of d/w=17.5 & 35, the inlet must be moved to expose a section of support which is in contact with the cold (figure 23). The minimum occurs when the recirculating fluid is cooled by this section and the temperature is transmitted through turbulent diffusion to the rest of the separated region. For the case of the wall off, the expected

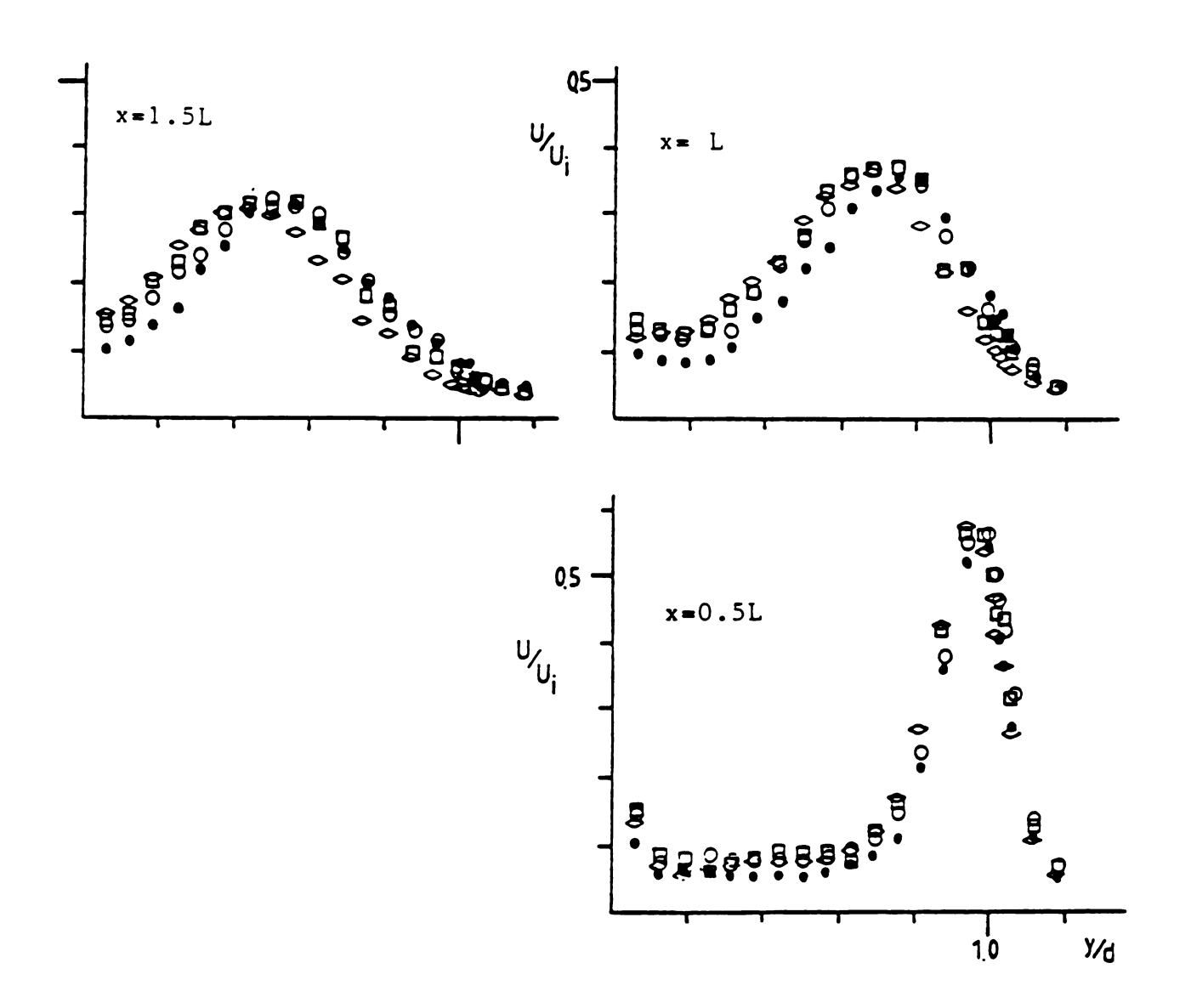


Figure 21 Velocity Profiles For Changes in Cold Wall Setting; $\Box - 5^{\circ}C$, $o - 10^{\circ}C$, $\diamond - 0FF$, $\bullet - 1$ sothermal.

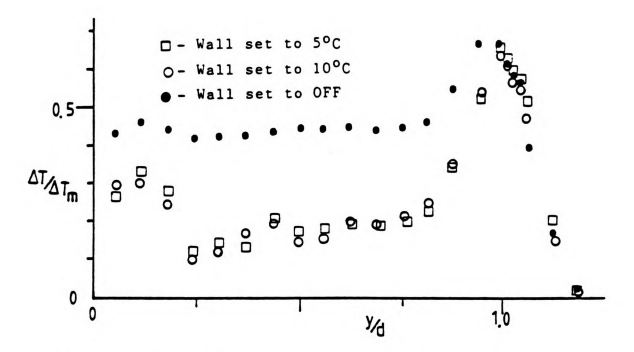


Figure 22 Velocity Profiles at 0.5L and Different Wall Temp.

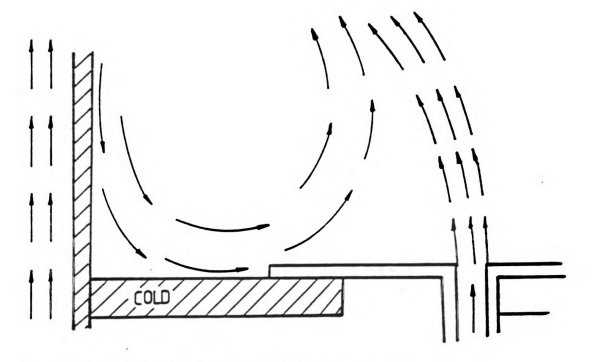


Figure 23 Flow Patterns Explaining Discrepancy

behavior of no temperature gradients in the separated region, /10/, is observed.

5.2.5 CHANGE IN REYNOLDS NUMBER

For this study, the geometry of d/w=10 is used with an inlet temperature of 27° C and the copper wall set to 10° C. Reynolds numbers of 3800,2600,2000, and 1200 are compared. The nondimensionalized velocity profiles show a difference only for Re=1200 (figure 24). This case seems to be developing more slowly and also with a higher peak velocity. When compared with the isothermal velocity profile, it appears that buoyancy is affecting the lowest Re to account for this difference. The differences in the nonisothermal jets disappears by the time they have developed into wall jets. No additional information is visible from the temperature measurements.

5.2.6 CHANGES IN SLOT WIDTH

From the data for reattachment lengths, it appears that this change in geometry does not greatly affect the overall motion of the flow. An increase or decrease in slot width by a factor of two accounts for only a 10% change in the reattachment distance. For this reason, the same measurement levels, grid lines, are used for comparison. The ratios of d/w=5,10 &20, which correspond to Re=7600, 3800, & 2000 respectively, are compared at a constant distance from the wall, d.

The velocity profiles show a decrease in peak velocity corresponding to a decrease in slot, and therefore jet,

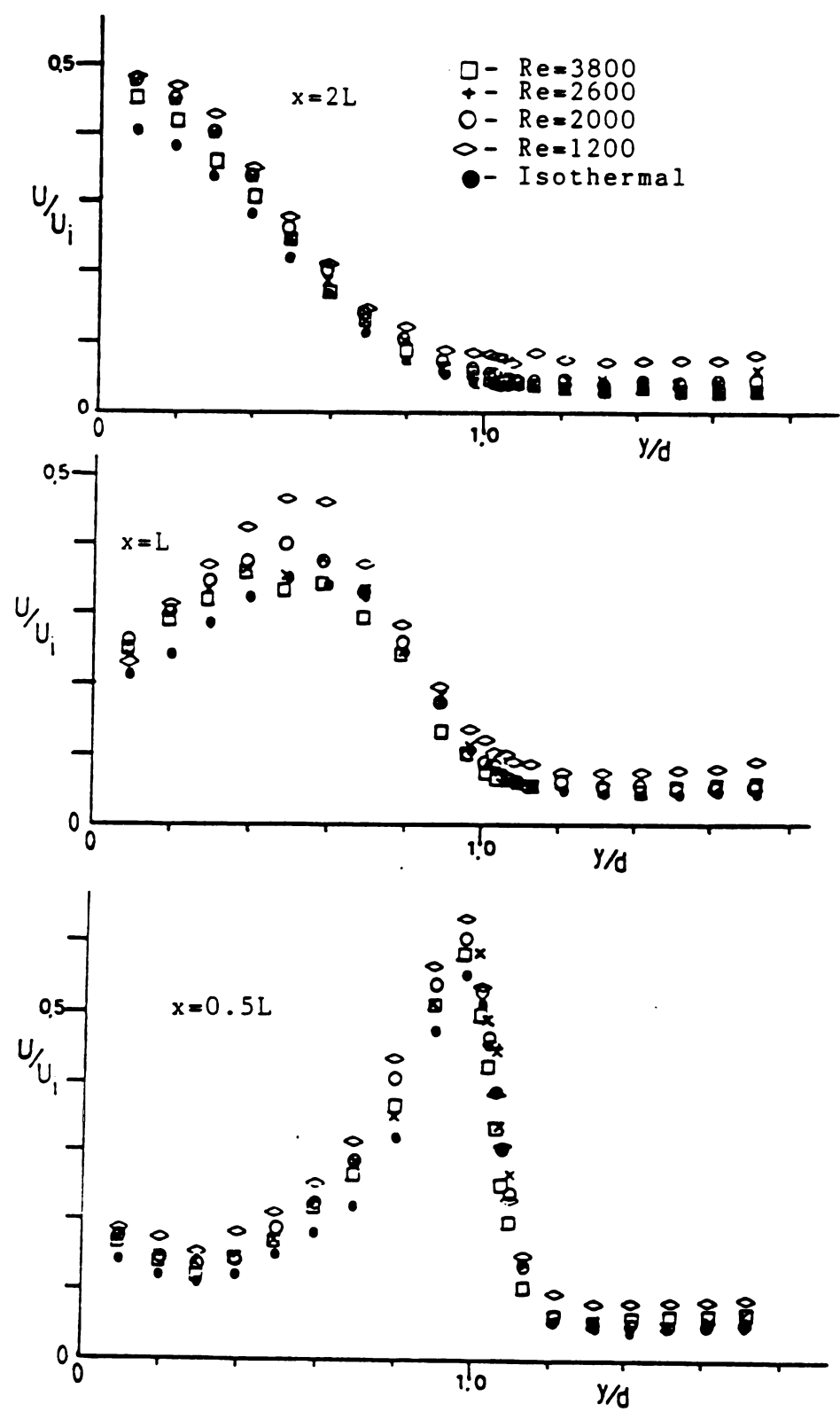


Figure 24 Velocity Profiles for Change in Re

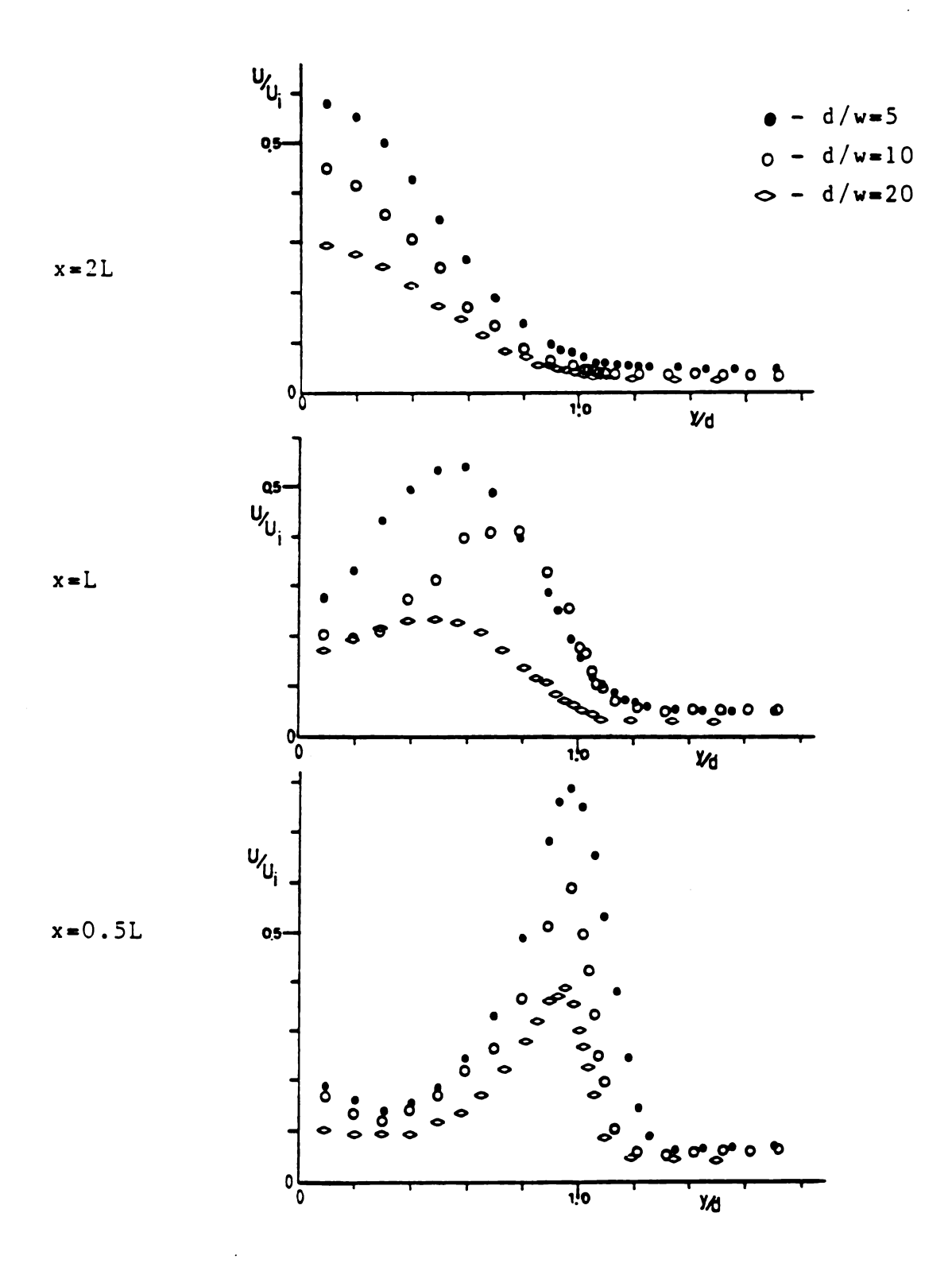


Figure 25 Velocity Profiles for Change in Slot Width

width(figure 25). This is expected as the shear layers reach the center sooner for a thinner jet, thereby diffusing momentum faster. The smallest slot width, d/w=20, appears to develop faster. with the largest, d/w=5, developing slowest. These small differences can be attributed to the fact that the separation distance increases with slot width. The smallest slot width therefore has a greater distance develop after reattachment to reach the same position. Due the measurement grid size, see APPENDIX A , comparisons at the same distance from reattachment possible.

All three of these geometries develop into a profile (figure 26) which can be made into an universal profile for a wall jet as found in the literature. /16-17/. This agrees with earlier work which showed the relaxation to a wall jet downstream of reattachment /1/. Deviation from the universal wall jet profile far from the wall is attributed to the ambient currents in the measurement chamber.

Universal profiles for temperature are also provided in the literature for a weakly buoyant wall flow with heat transfer /18/. The present data indicates that for these cases, the temperature profiles are also developed and that of a wall flow. (figure 27) The differences in the region close to the wall between the present data and that of Faeth and Liburdy is attributed to the higher temperature difference between the jet and the wall than in the previous study. The previous data was made with the wall initially at ambient temperature where the present study has the wall below ambient.

While the universal profiles are useful confirming the development of the wall jet, they eliminate differences in

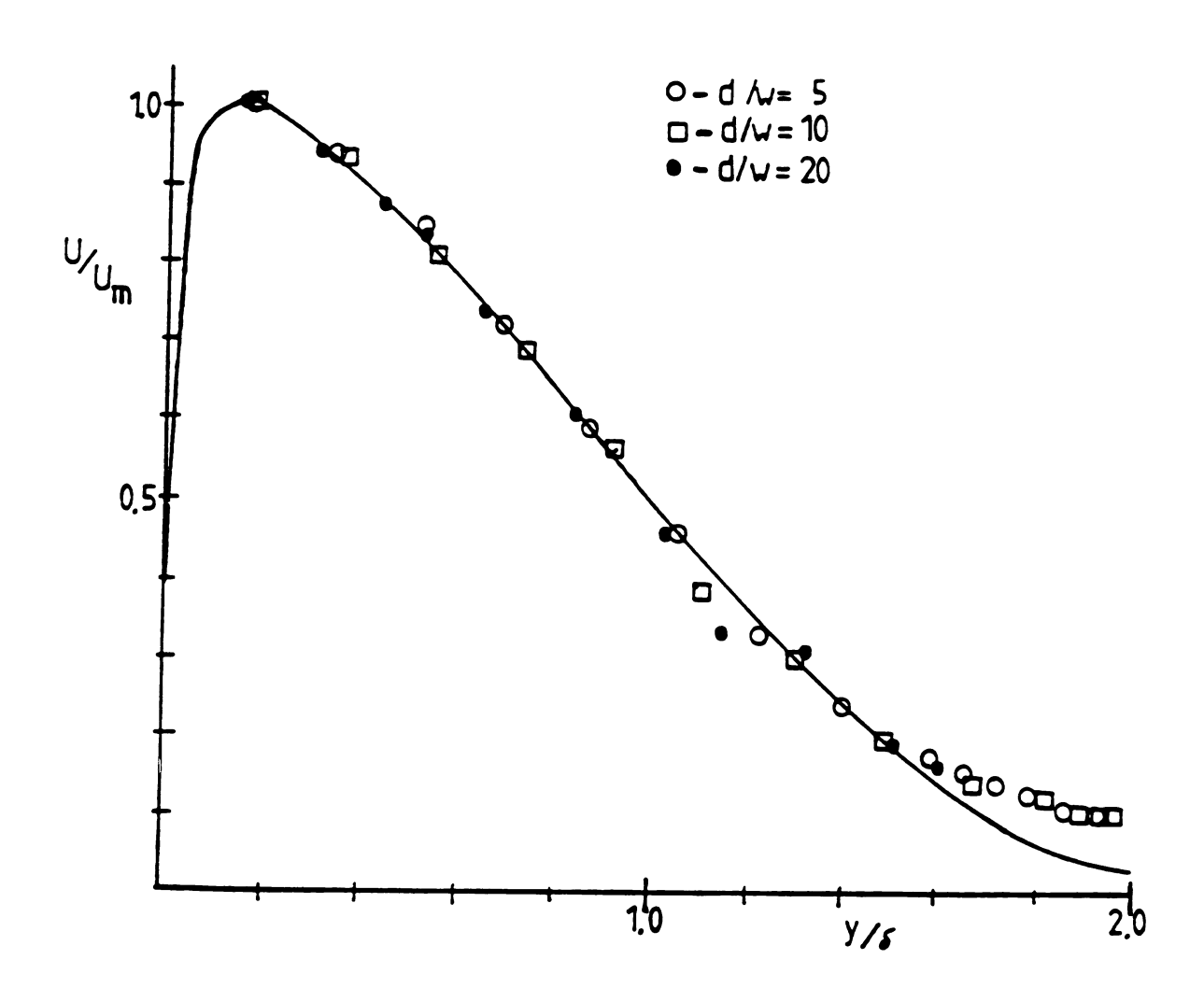


Figure 26 Universal Velocity Profiles for a Wall Jet /16-17/

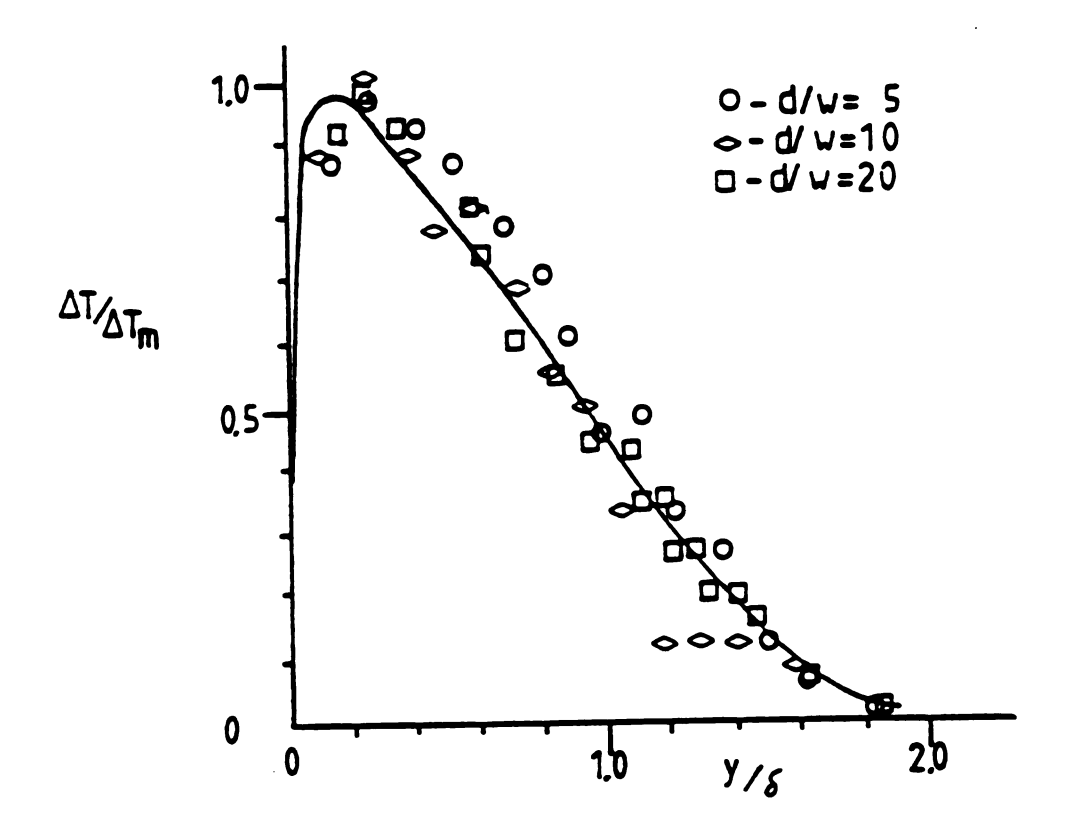


Figure 27 Universal Temperature Profile /18/

magnitudes of the profiles. When the developed velocity profiles are compared in magnitude with the isothermal velocity profile for each respective case, some differences are shown (Figure 28). The case of Re=3800 was previously shown to have a peak velocity about 15% higher than the isothermal case. For a Re=7600, the difference disappears. For this case, the momentum forces are the only significant forces and buoyancy plays no role to this point in the flow. For the case of Re=2000 it was shown previously (fig. 24) that for a constant slot width there was no difference between that and the case for Re=3800 yet the differences in peak velocity is much less. This may be a result of the grid size rather than an actual physical phenomenon. The closest grid point to

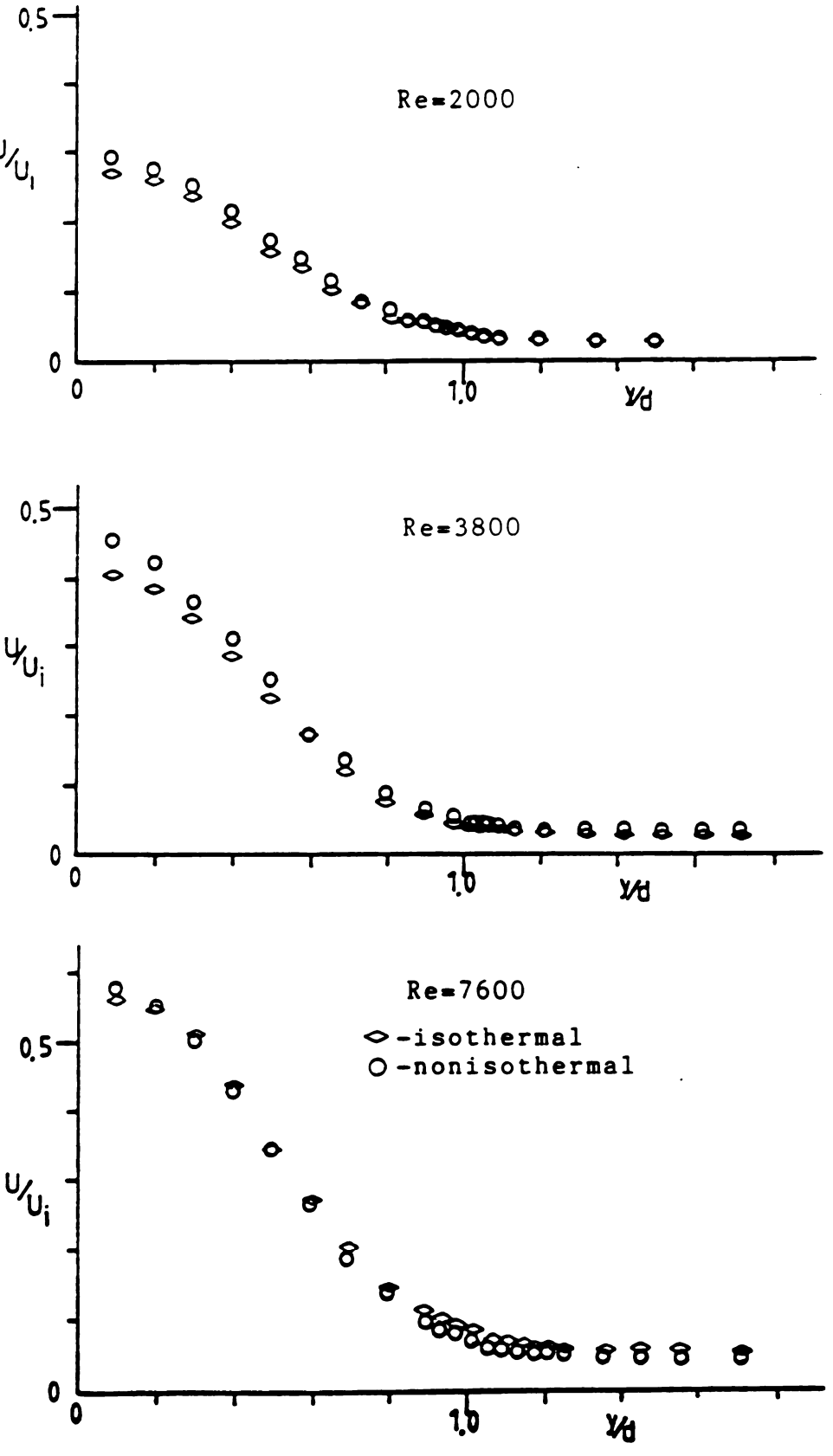


Figure 28 Isothermal and Nonisothermal Velocities at 2L

the wall for Re=2000 is 2w, two slot widths, from the wall where it is w from the wall for Re=3800. The peak velocity for the lowest Re may be between the closest grid point and the wall. More confidence is held in the highest Re where only 0.5w separates the wall and the first measurement point.

5.2.7 CHANGE IN STEP HEIGHT

When comparing flows with differing distances between jet and the wall, step height,d, care must be taken. It was earlier that the flows are very different with separation distances varying by 50%. For this reason, comparison of the same measurement lines is not meaningful since they would be comparing different stages in the The separation distance. L, is therefore to nondimensionalize the distances These downstream. nondimensional distances are then compared. Re=3800 was used for the comparison with d/w=10 & 17.5 chosen to match the slot widths. w.

The velocity profiles show differences developing as early as 0.55L where the d/w=10 case shows more spreading toward the wall. (figure 29) This difference is also visible at L where the bulk of the jet for d/w=17.5 is much farther from the wall. Even when the 1.4L position for the 17.5 case is compared with the profile for the 10 case at L, the former appears to be lacking in development. This difference is still visible when closer d/w ratios are used, 20 and 17.5 and Re are matched at 2000 (figure 30). This indicates that the development is much slower at the stages immediately after reattachment.

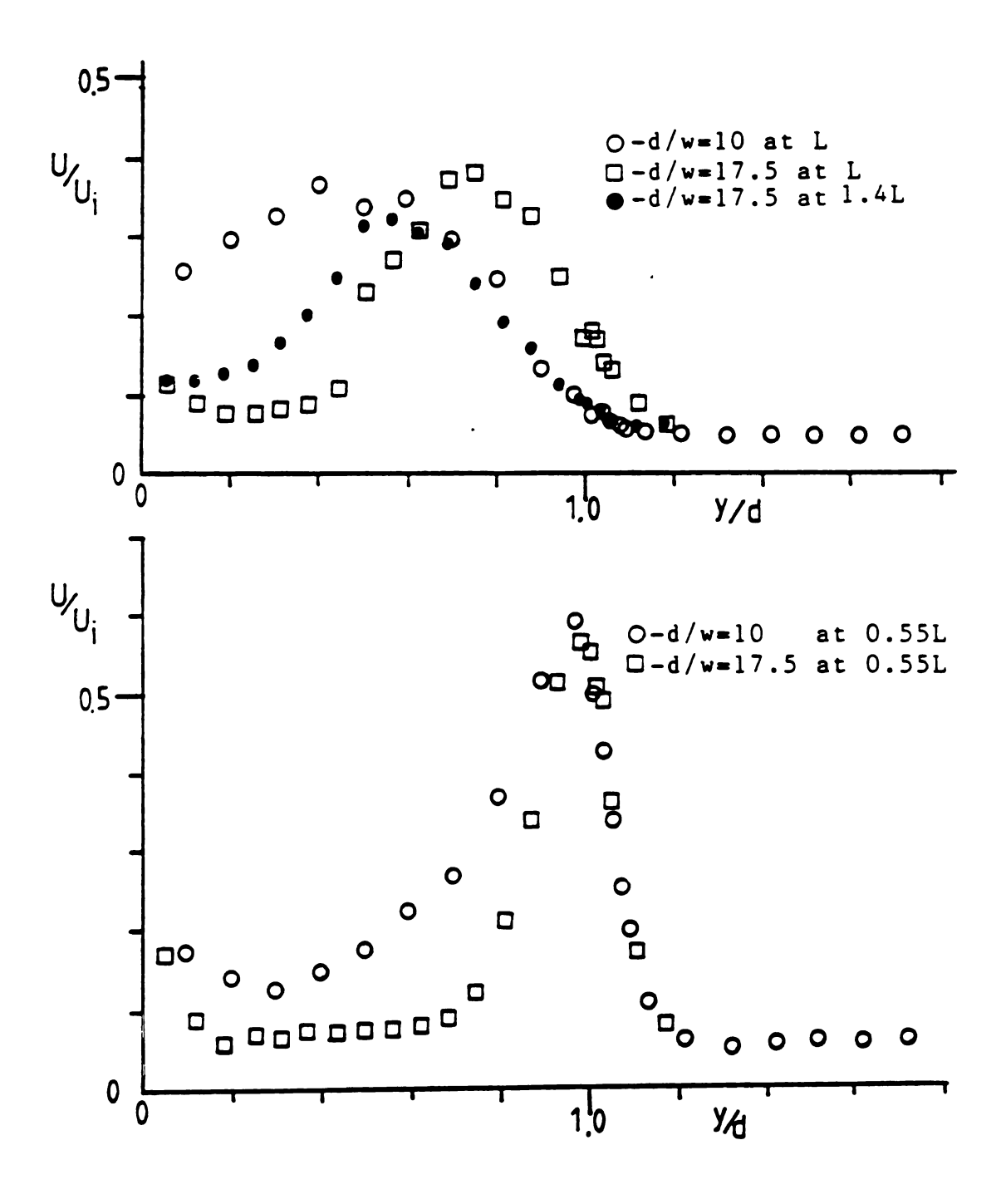


Figure 29 Velocity Profiles for Changes in Step Height

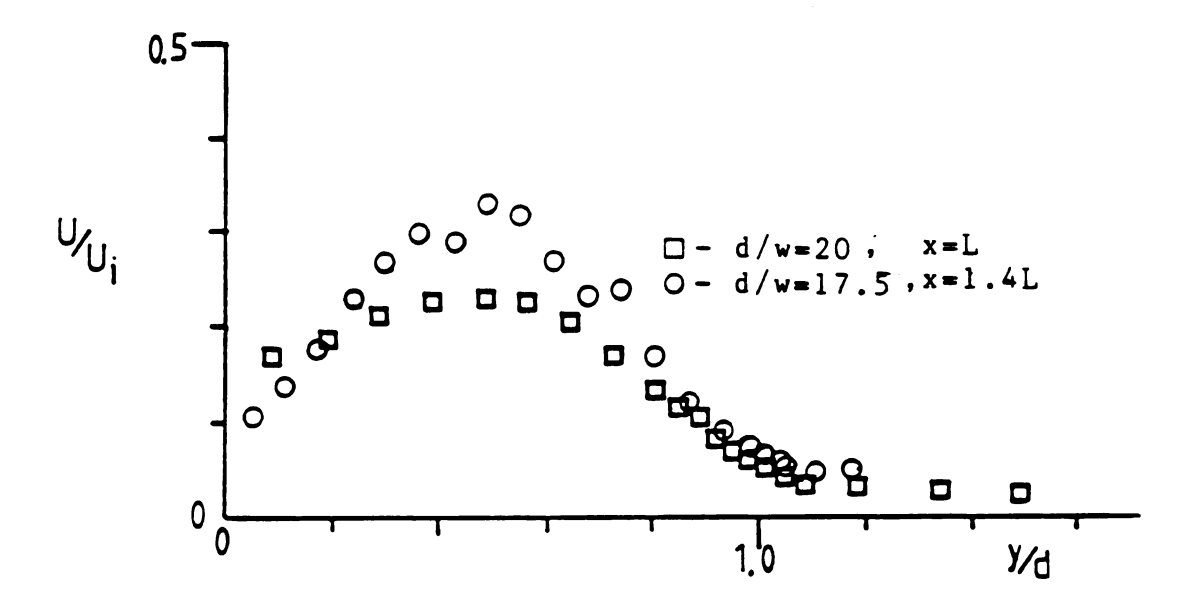


Figure 30 Velocity Profiles for Change in Step Height

Another interesting observation about figure 29 is that at the reattachment point, the peak velocities are close to the same. Since the case of d/w=17.5 travelled 50% more slot widths to reattachment, the expectation is that the peak should be 20% lower than that for the d/w=10 case. (4) This may be due to the fact that there is much mixing and reorienting of momentum at this point and that a true peak or centerline velocity can not be meaningfully compared.

The differences in the development of the different heights may mean that the redevelopment of the case of d/w=17.5, when it takes on the characteristics of a wall jet, is further downstream than the 1.6L found for the cases of d/w=5.10 & 20.The comparison of the latter showed that the width was not an important dimension redevelopment length. This leaves the reattachment and step height as possible governing length scales. profile for d/w=17.5 at 1.3L shows little development toward a wall jet which may indicate that this is not the most important length. Clearly, redevelopment can not occur until after reattachment and therefore any characteristic

should be measured from this point. The d/w cases of 5,10,20 all redeveloped within two step heights after reattachment. If this scale is used for the d/w=17.5 case, the last grid measurement was made at one step height downstream of reattachment. This allows a greater distance for redevelopment which this case clearly needs. Unfortunately, due to restrictions of the test equipment, the developed region for this case could not be measured to test this length scale for the larger step heights. The latter scale seems the most appropriate since it allows for a greater distance to redevelop for the larger step heights and fits with the data for the smaller step heights.

5.2.8 CHANGES IN ANGLE OF JET

An angle of 15 degrees away from the wall was used to compare with the data for the parallel cases. The slot width, w, and step height, d, were matched with the case of d/w=10. The angle resulted in a doubling of the separation distance. For this reason, the length scale of the separation distance is used for comparison of velocity profiles. (figure 31)

The profiles show nothing unexpected when compared with those of the parallel case. At 0.5L the profiles look similar with the angle case having a larger separated region but the basic characteristics being the same. At the reattachment point, the profile for the angle is more spread out and has a lower peak velocity. These are in agreement with expectations since the case for the angle travels twice as many slot widths as a free jet and therefore dissipates more momentum. The difference in the peaks, 30%, is in agreement with the expectation for a jet which travels twice the distance./4/ Temperature profiles also show the same basic characteristics for the two cases.

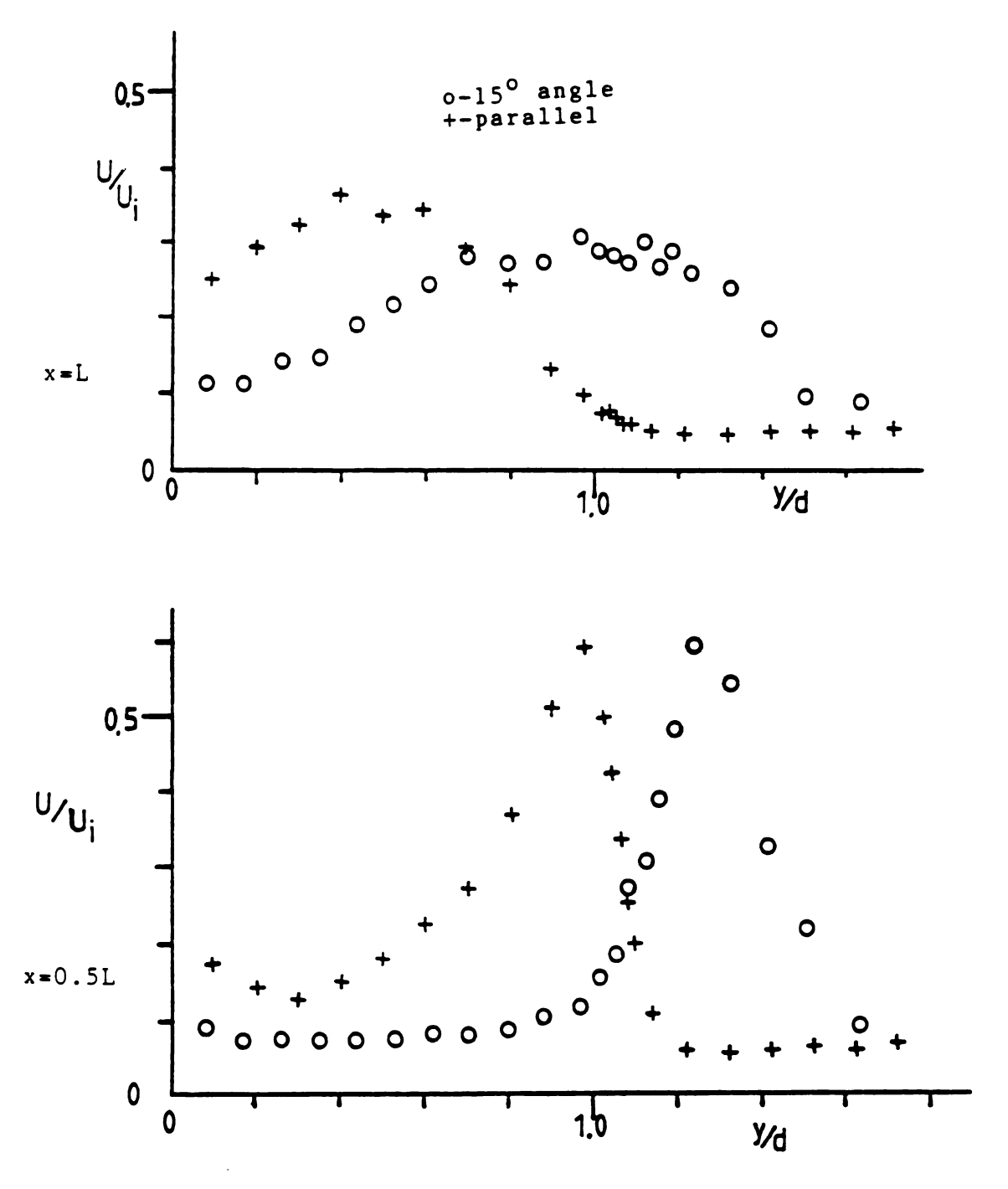


Figure 31 Velocity Profiles for Different Jet Angles

5.2.9 WATER VAPOR CONCENTRATION

Water vapor concentration levels were measured at each grid point. Due to a problem in the data acquisition, only the results for the geometry of d/w=10 are available for analysis. Earlier work showed that the inlet conditions for the jet wandered somewhat during a measurement period. /27/ The concentration levels at the respective grid locations show a very high sensitivity to the inlet condition. The inlet concentration level was measured only at the beginning of each measurement set. This can be used to normalize the profiles, which brings them somewhat into line with one another for the first few grid lines. Trends in later grid lines are unclear since the variations in the inlet condition are of the same magnitude as any possible trends.

Basic characteristics of the profiles show nothing unexpected. (Figure 32) The high gradients are located in the shear layers of the jet. The separated region has a slight gradient across it. This comes from the recirculating fluid near the wall having a higher moisture level than the inlet. The result is that the recirculation zone has a concentration level between that of the jet and the ambient. After reattachment the area near the wall stays at a subambient level but increases in the streamwise direction as mixing with the ambient increases.

One trend that can be seen from the profiles is that the gradients are less severe with decreasing Reynolds number. At the lower Reynolds number, diffusion becomes a more important factor in the distribution of water vapor, resulting in less sharply defined regions of high and low concentration.

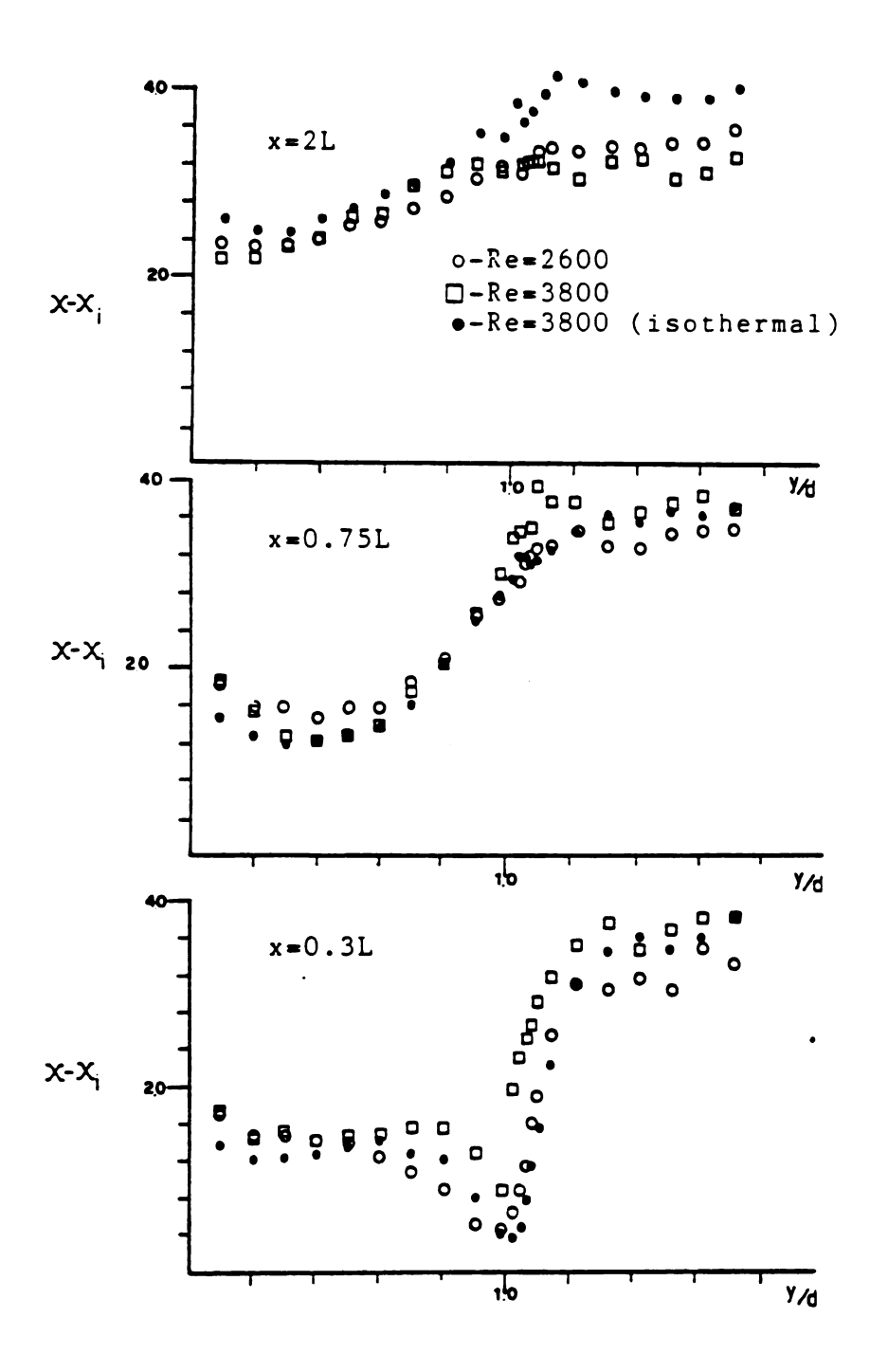


Figure 32 Water Vapor Concentration Profiles

5.3 COMPARISON WITH COMPUTER PREDICTION

The measured data for the separated and reattaching zones compared with the computer prediction mentioned previously /19/. Care must be taken when comparing measurements with the predictions as there are several difficulties in direct comparison. One is that the program gives values for velocity components where as the measured data is for the velocity magnitude. Because a staggered grid is used for the computation /21/, the velocity components are given for different locations and are therefore not easily converted to one magnitude for a single point. problem in comparison is that wall functions are used for the The first grid point for the near wall region. corresponds roughly to the second measurement grid point. Difficulties mentioned previously with the measurement are therefore magnified with the computer grid in the wall region. In other regions, separation distance between lines is great compared to the length scales of This results from the fact that the grid is used predicting the characteristics of the entire room and therefore based on these length scales. To overcome problem, a finer grid was used for the case of d/w=10 Re=3800.The results are compared to those for the larger grid. Both the measurement and computer grids still distances between grid lines which make comparison in areas of high gradients difficult. The final problem involves temperature information. Because of discrepancies between the predictions and measurements in the room, factors were added to the heat transfer coefficients and thereby effected the temperature profiles. The result of this is that the comparison of temperature profiles gives no significant information. For this reason, the comparison is limited to reattachment and velocity information.

5.3.1 REATTACHMENT LENGTHS

Reattachment lengths for the computer predictions difficult to determine. Not only is the closest grid point to the wall is of the order twice the slot width of the jet, but the distance between grid lines is of the order of 0.8d. Keeping in mind that for the case of d/w=10, the separation distance was 2.2d, this is a large distance. A finer grid for the case of d/w=10 was used to compare with the standard grid in which the distance between lines was only 0.2d. showed that the interpolation method for finding the points of reattachment for the other cases was a good approximation. The method used for finding the reattachment point locating the point of zero velocity in the flow direction, or the point where the sign of the u component of velocity changed from positive to negative. This was done by linearly interpolating between grid lines of opposite signs for velocity. The point located was the position of the dividing streamline at the first grid line. Since the streamline passes this point at an angle with respect to the wall, true point of reattachment would be located further upstream. To approximate this, an angle of 45 was assumed between the point on the grid line and the wall. These results are compared to the measured points and those calculated using the equation (2.1) from Regenscheit /4/ for a normal coanda jet. (Table 3)

TABLE 3 Reattachment Lengths

d/w	Measurement	Literature /4/	Computation
10	22	17	16
20	19	15	16
17.5	32	27	27
10*	39		26

*- 15 degree angle

When the case of d/w=10 was compared to that for a finer grid where the grid spacing was only 0.2d, the agreement was In fact, to the accuracy of 0.1d, the accuracy of the measured results, the points were the same. A second way to check the reattachment point was also used. The Stanton number peaks near the reattachment point, as stated earlier /10-12/. The computer prediction shows a definite maximum at, or near the reattachment point. When the peak in the Stanton number was found for the finer grid, it corresponded to 1.5d. This agrees well with the estimate for the reattachment point of 1.6d. In fact, Vogel and Eaton /11/ found that the peak Stanton number actually occurs on the order of 0.1L upstream of the reattachment point. While these estimates do not claim to be that accurate, it shows that for comparison purposes, they are a good approximation.

When the results are compared in table 3, the computed results show lower values than that for the measured data. The largest discrepency is in the case of the jet issuing at an angle from the wall. Literature data is not available to compare for this case. For the other cases listed, the program agrees well with the previous studies for a coanda jet. The measured data are however above these values. This

indicates that the computer program does not respond well to the ambient currents effecting entrainment and pressure gradients as discussed earlier for the measured reattachment points.

5.3.2 COMPARISON OF VELOCITY PROFILES

As mentioned previously, care must be taken to compare velocities which are primarily of only one component. The v components of velocity in the prediction become negligible after reattachment when the jet begins to redevelop. Comparison is therefore limited to this region.

the profiles for the case of d/w=10 and Re=3800 compared at a height of 4.5d using the two grid sizes, differences appear (figure 33). The magnitudes of the peak velocity is slightly higher, 6%. The shape for the finer grid is much closer to that of the developed jet. It should be noted that the change in shape is much greater on the free side of the jet than that close to the wall. In fact the position of the first three grid points for each case relative to each other changes only slightly. This indicates that the wall functions used as a boundary condition may source of discrepency. The functions used are based logarithmic law-of-the-wall /19/ which is correct for parallel or nearly parallel flows /24/. In the reattaching region, the flow is clearly not parallel. Another factor suggesting that this is an area of trouble is that the peak velocity in the measurements occurs between the wall and the first computed grid line. The wall functions assume a constant shear stress across this region. Since a maximum in velocity corresponds to a change in sign of the shear stress

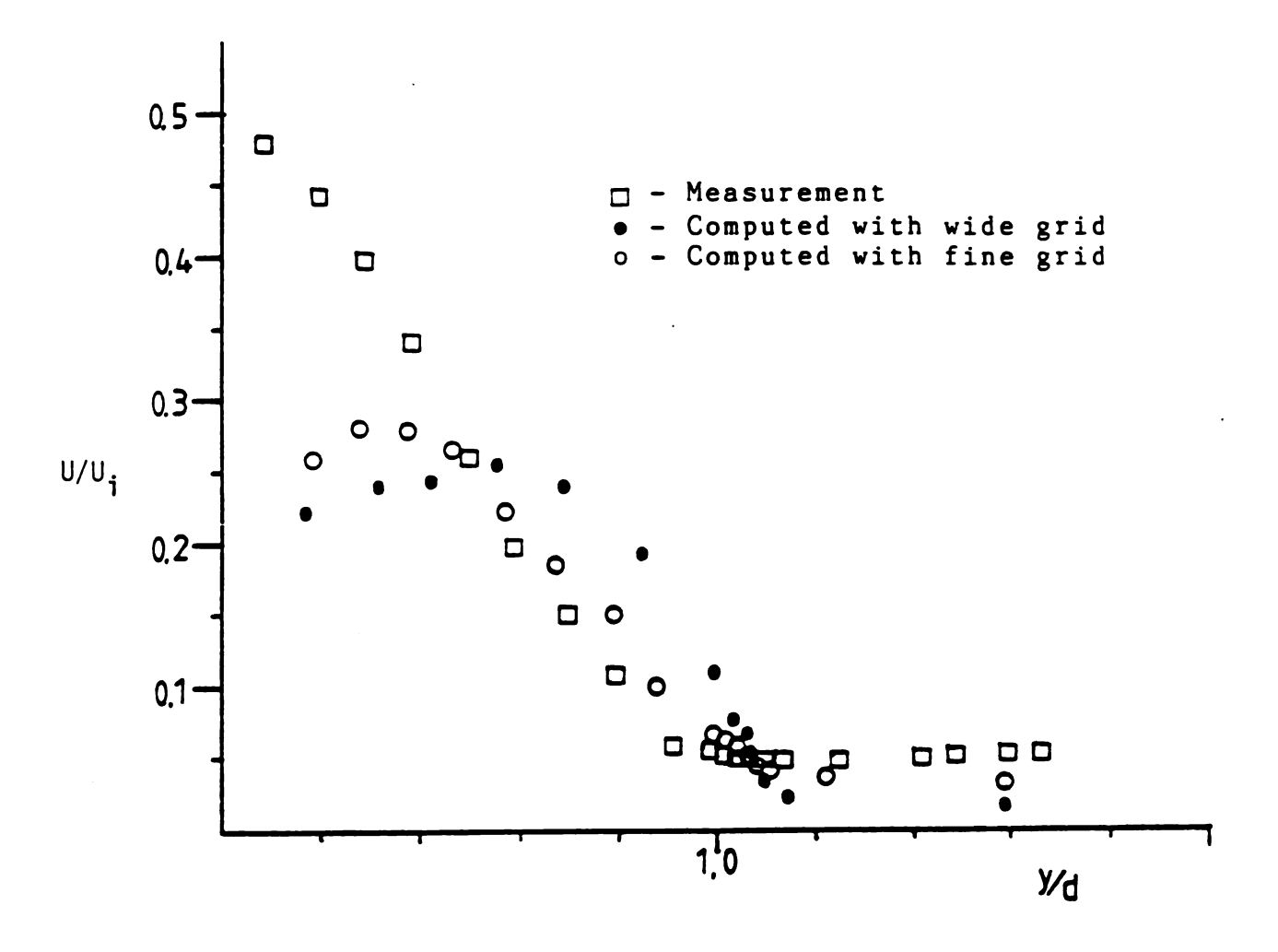


Figure 33 Velocity Profiles at 2L, (measured and predicted)

as well, this is clearly in error. The extent to which these contribute to the discrepency between prediction and measurement is not clear and could only be determined by examining the near wall region.

Both the magnitude and shape of the predicted profile are different from the measured results. While the shape of the predicted velocity is similar, it is clearly not the profile of a developed wall jet. This is illustrated by comparing it to the universal profile (figure 34). This profile, though

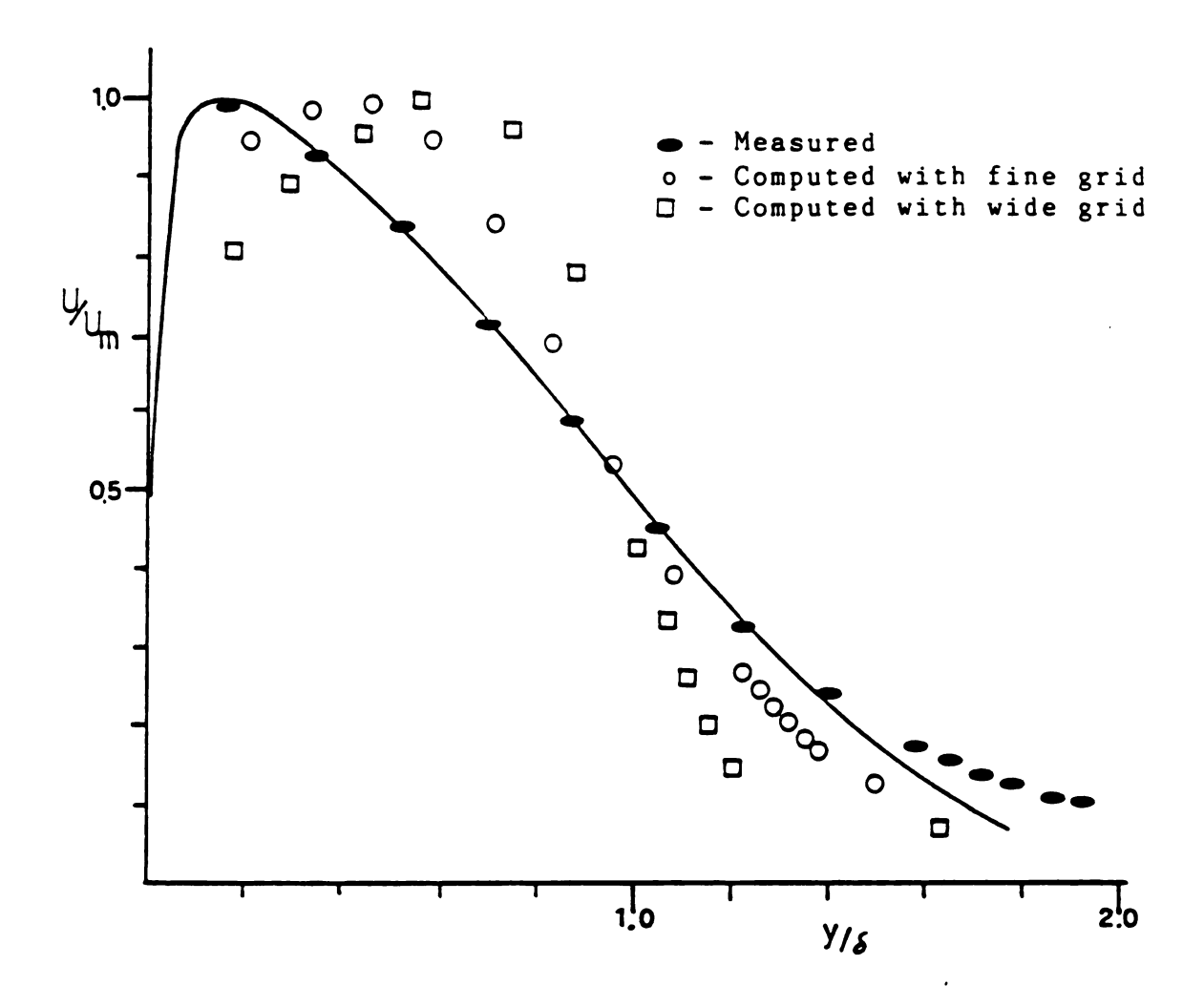


Figure 34 Universal Velocity Profile /16/ at 2L

not that of a wall jet, has developed into a nearly parallel flow to the wall as illustrated by the lack of components of velocity perpendicular to the wall. This also points to the wall functions as a boundary condition being a source of problems, not allowing the jet close enough to the wall due to the constant shear stress assumption.

The magnitude of the prediction is much less than that of

the measurement. The magnitude of the peak can easily be estimated for an expected value. A reattaching jet is a free jet for part of the flow and later becomes a wall jet. Since the decay of peak velocities is well known for both cases /4/, an estimate can be made based on the distance travelled in both states. The separated path length is estimated using the quarter perimeter of an ellipse /22/;

$$1 = \pi/4(1.5 (a+b) - \sqrt{ab})$$
 5.1

where 1 is the distance travelled and a and b are d and L respectively. This distance is then added to the distance from the reattachment point to the point of comparison. The results are shown in table 4. Data from Sawyer is also

TABLE 4- Comparison of Centerline Velocity Magnitudes

	Distance (w)	Free Jet (u/u _i)	Wall Jet (u/u _i)	Coanda Jet (u/u _i)
Measured	49.0	0.38	0.53	0.48
Sawyer	19.2	0.44	0.60	0.56
Computed	49.7	0.37	0.53	0.30

compared. The result shows the present data as well as that of Sawyer to fall within the expected bounds. In fact both fall closer to a wall jet. The computed results fall out of the expected range, below the lower bound of a free jet. Fecause the reattachment length was shorter for the computed flow, and therefore a greater portion was spent as an attached flow, this result is even more surprising.

It seems clear that the predicted jet has less momentum and a different profile to that of a wall jet at the point comparison, 4d downstream of the jet inlet. A momentum loss in the jet is therefore in the separated or reattaching zone, or both. The wall functions have already been discussed as a possible source of discrepency. This is not the only The velocity profiles show a zone possibility however. opposing flow on the free side of the jet while separated . This may be another factor reducing the momentum of the jet since it would act as a sink for momentum increasing the shear stresses on the free side. It was not determined if this region exits in the same proportion in the experimental facility. The measured data unfortunately gives information of the sign of velocity necessary for such a Problems with the turbulence model itself possible in this area. The $k-\varepsilon$ model assumes isotropic turbulence which is definitely not the case in the area Streamline curvature which is not taken into reattachment. account in the present model can have significant influences on the flow /6/. In the recirculation zones, the streamline curvature is very great. It is possible that too much energy passed to the recirculation zones accounting for loss. Gooray et al./15/ showed that observed the recirculation area could be modelled taking these effects

into account. A more detailed analysis of the jet region, especially the near wall region would be required to answer these questions.

The question of whether or not the computed jet will develop into a wall jet downstream also remains. This can only be answered by comparing results at distances farther downstream.

5.4 WALL JET REGION

order to make comparisons with the computer program at positions farther along the wall, measurements were done with the equipment used for room air measurements. (see EQUIPMENT PROCEDURE) Velocity profiles were made at positions 15d, 20d, 25d, and 30d along the wall for cases of d/w=10 and Re=3800 and 2600. These were done with the cold wall on and inlet temperature of 27°C as well as an isothermal case where the wall was turned off.(see EQUIPMENT AND PROCEDURE) The results showed no difference in the two Reynolds numbers. The computed results consistently fall below those for measurements (figure 35). There is a better agreement in the overall shapes of the profiles than closer reattachment zone. The region close to the wall appears be different, but this region is difficult to compare due to the distances of the first grid points. The computed results show a profile which is close to a universal wall jet profile (figure 36). The profile does not go to zero because of the currents of the room parallel to the jet. For this reason, a be made up to comparison can only an approximate nondimensional value of y=1.1. In this region there is much better agreement than closer to the reattachment point.

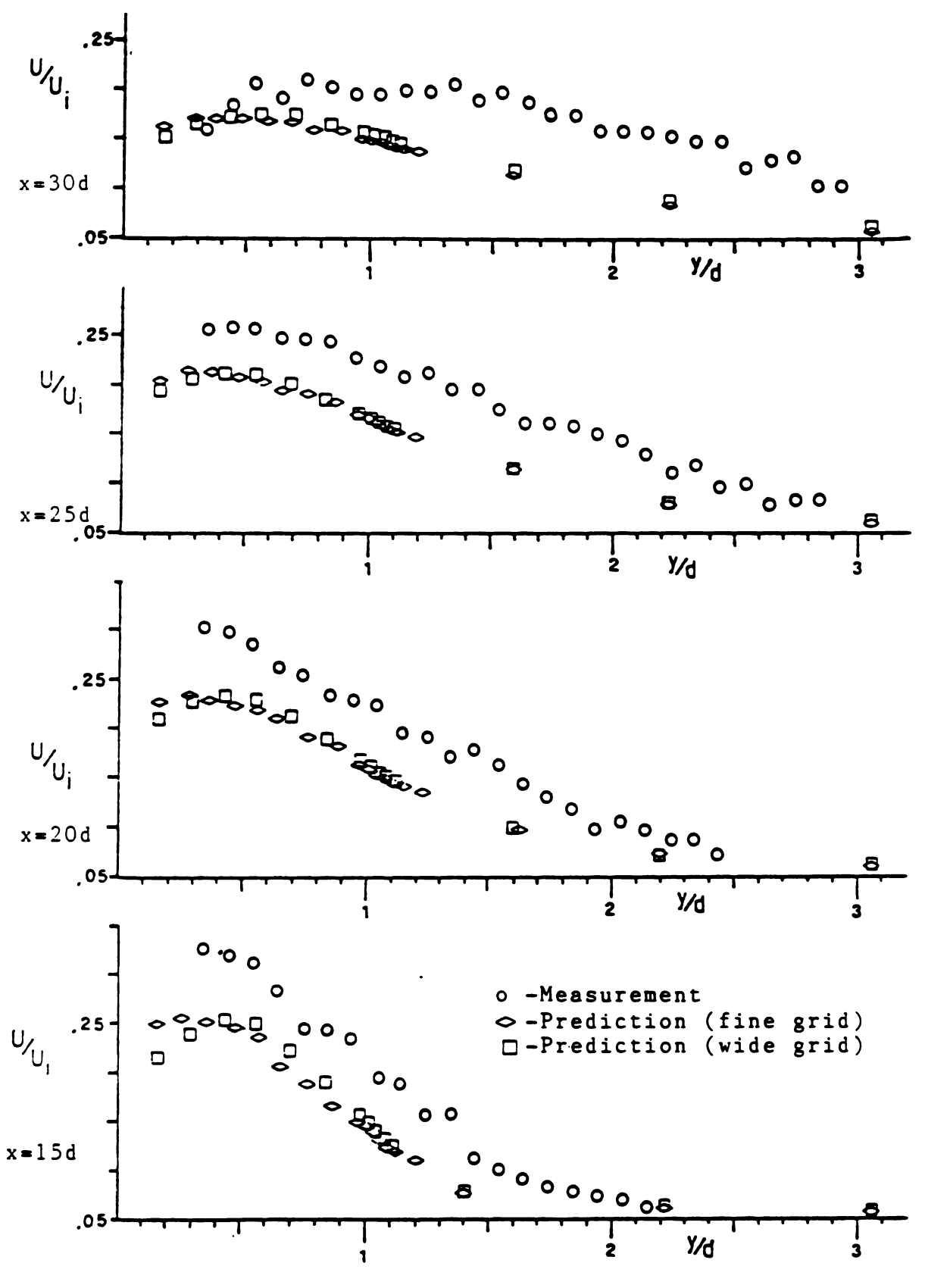


Figure 35 Velocity Profiles

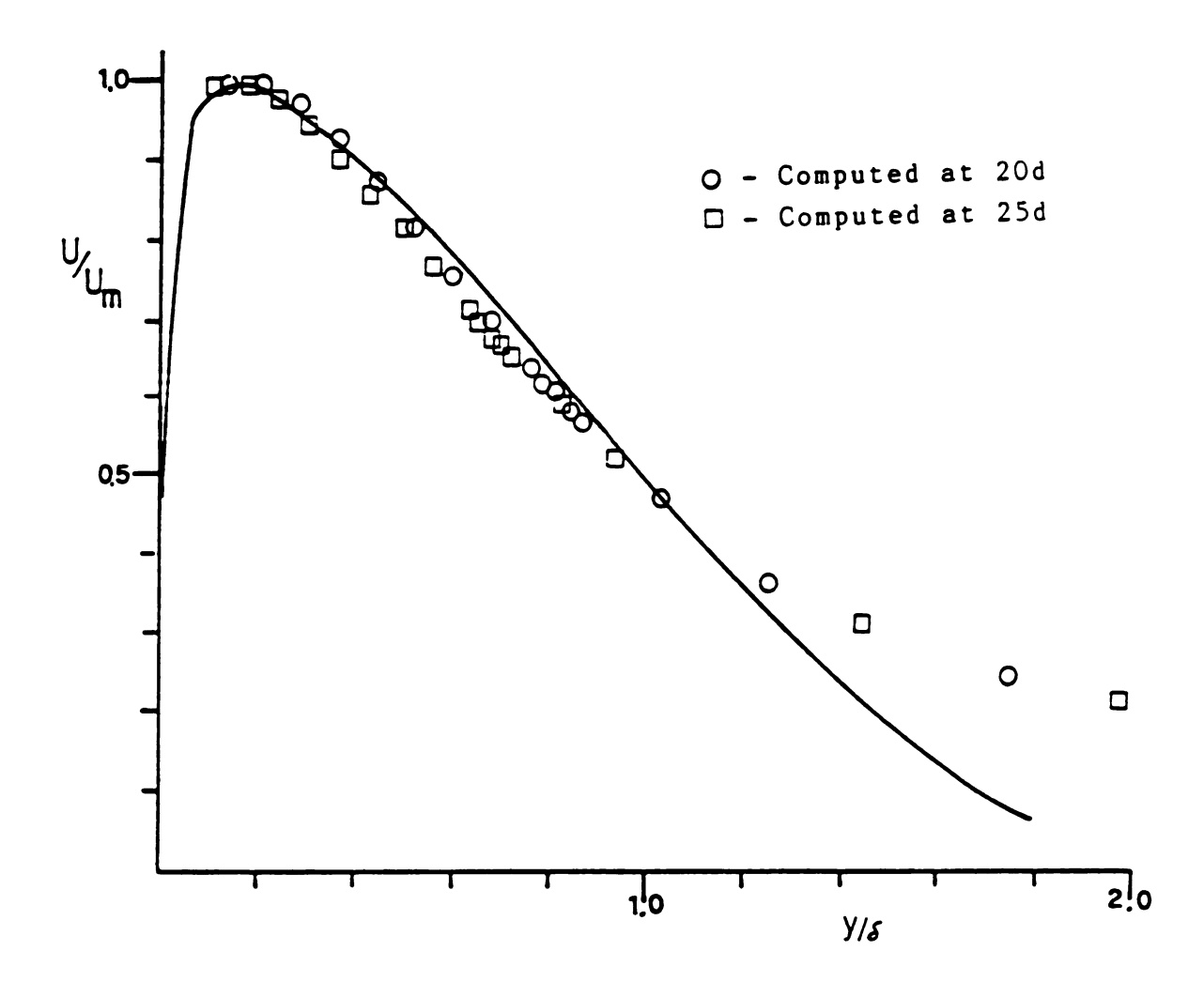


Figure 36 Universal Velocity Profile /17/

It can be seen from figure 35 that while the finer grid greatly affected the shape of the velocity profiles in region of reattachment, there is only a small effect at the downstream locations. The large scale behavior of the jet seems equally well described by either grid. This agrees with earlier work which stated that the grid size in the jet would not affect the predictions for the entire room /19/ since the necessary information is supplied by the larger

grid size.

behavior of the jet was similar when comparing isothermal to nonisothermal cases for the measurements and predictions (figure 37). When compared to isothermal case, isothermal velocities decreased near the wall increased on the free side. This is a result of the fluid near the wall being cooled by the wall and having buoyancy acting against the momentum. On the free side, the ambient temperature is lower than that of the jet and the therefore positively effected by buoyancy. This indicates that the program responds correctly to influences of buoyancy forces and its effects on momentum in the developed region. The wall jet region indicates that the computer program capable of predicting the behavior of a wall jet to a reasonable degree of accuracy, in agreement with Schmitz /19/. The analysis in this region points back reattaching region as the source of discrepency experiment and prediction.

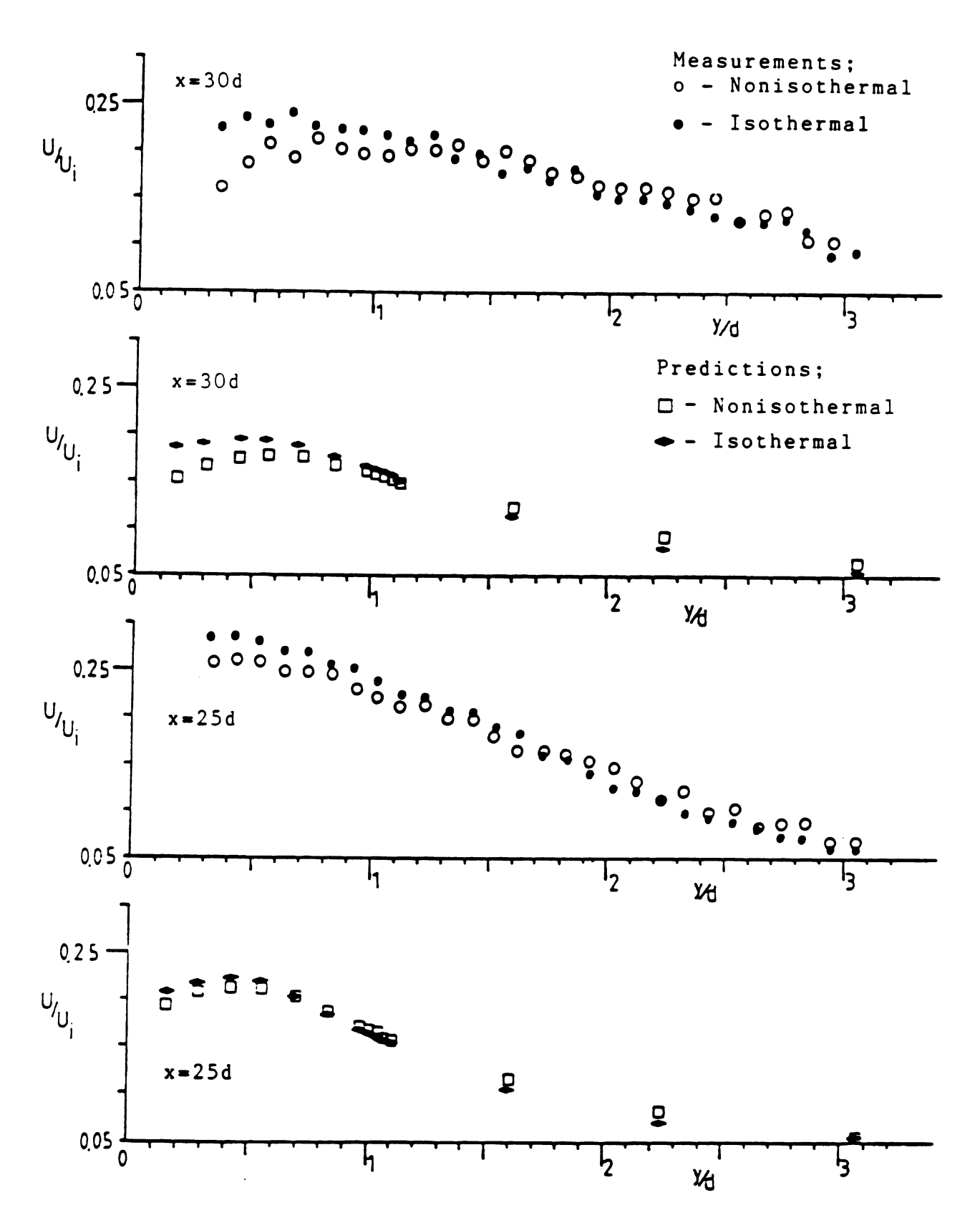


Figure 37 Wall jet velocity profiles for non- and isothermal

6. CONCLUSIONS

The air jet under study provides a suitable inlet condition for the measurements of the room air distribution. Block or parabolic inlet profiles approximate the actual profiles to a reasonable degree. The flow is fully turbulent in the separated region for Reynolds numbers as low as 1200 as observed by the constant reattachment distances. Two dimensionality is good for the velocity field and the general flow pattern. A temperature gradient which is observed at the inlet disappears within the first 15% of the wall flow.

Reattachment lengths of the jet are affected by the experimental apparatus, resulting in larger than expected values. This effect comes from the ambient currents in the measurement chamber. The inlet structure may influence the entraining flow pattern as observed in the computer prediction. The extent to which each contributes to these is not clear at this time.

For a given geometry, the variation of system parameters has no significant effect on reattachment distances. The step height was the significant dimension for determining the reattachment location. Slot width had an effect also, although a much smaller one. The exact location of the reattachment point fluctuated on the order of 1/10 the distance to reattachment. An angle of 15 away from the wall increases the reattachment distance by a factor of 2.

Because of an interdependence of the operating parameters (inlet temperature, wall temperature, inlet flow rate, ambient temperature) on one another, isolation of one parameter is difficult. It is apparent however that in the reattaching zone, these have little or no effect. When nonisothermal conditions are compared to the isothermal case,

there is a difference for Reynolds numbers less than 4000. This difference appears as higher peak velocities for the nonisothermal cases. The difference is the same for Reynolds numbers down to 2000 where the effect becomes larger. The geometry of the flow is the overriding factor in determining the flow characteristics.

The reattaching flow develops into a wall jet within 2d after reattachment for the geometries which allowed this location to be measured. Temperature profiles are also fully developed at this point.

The computer program does not predict the flow well in the reattaching region. Both the shape and the magnitude of the velocity profiles are predicted wrong. The grid size has an effect on the shape but little on the magnitude. The magnitudes are well below expectations. The peak velocities are much further from the wall than observed in measurements. This is a result of the wall functions used in the program as a boundary condition.

A momentum deficit occurs within the first 0.5 meters of the flow in the program when compared to the measurements. This indicates that the dissipation in the program is too high. It is unclear as to the exact cause ,however it occurs in a region of the flow where many of the assumptions of the model used are not valid. The loss occurs either in the separated or reattaching region or both. Determining the exact reason and location of the momentum loss would require much more extensive analysis of the computer program as well as a more detailed examination of the experimental flow field.

The computer predictions for the upper regions of the wall flow are much better although they still exhibit this same

momentum deficit. The size of the computation grid has very little effect on the shape or magnitude of the velocity profiles in this region.

The overall behavior of the jet is predicted well for majority of the wall flow. The inital region is a source of The correction of this error requires changing computational model and more detailed experimental information than is possible with the present facility. corrections in the model necessary to bring the prediction in agreement with the measurements may not be economical efficient when considering the computations for the entire It does not seem possible however that the predictions for the room could be made accurately when the driving force of the room flow is not accurately predicted.

APPENDICES

APPENDIX A

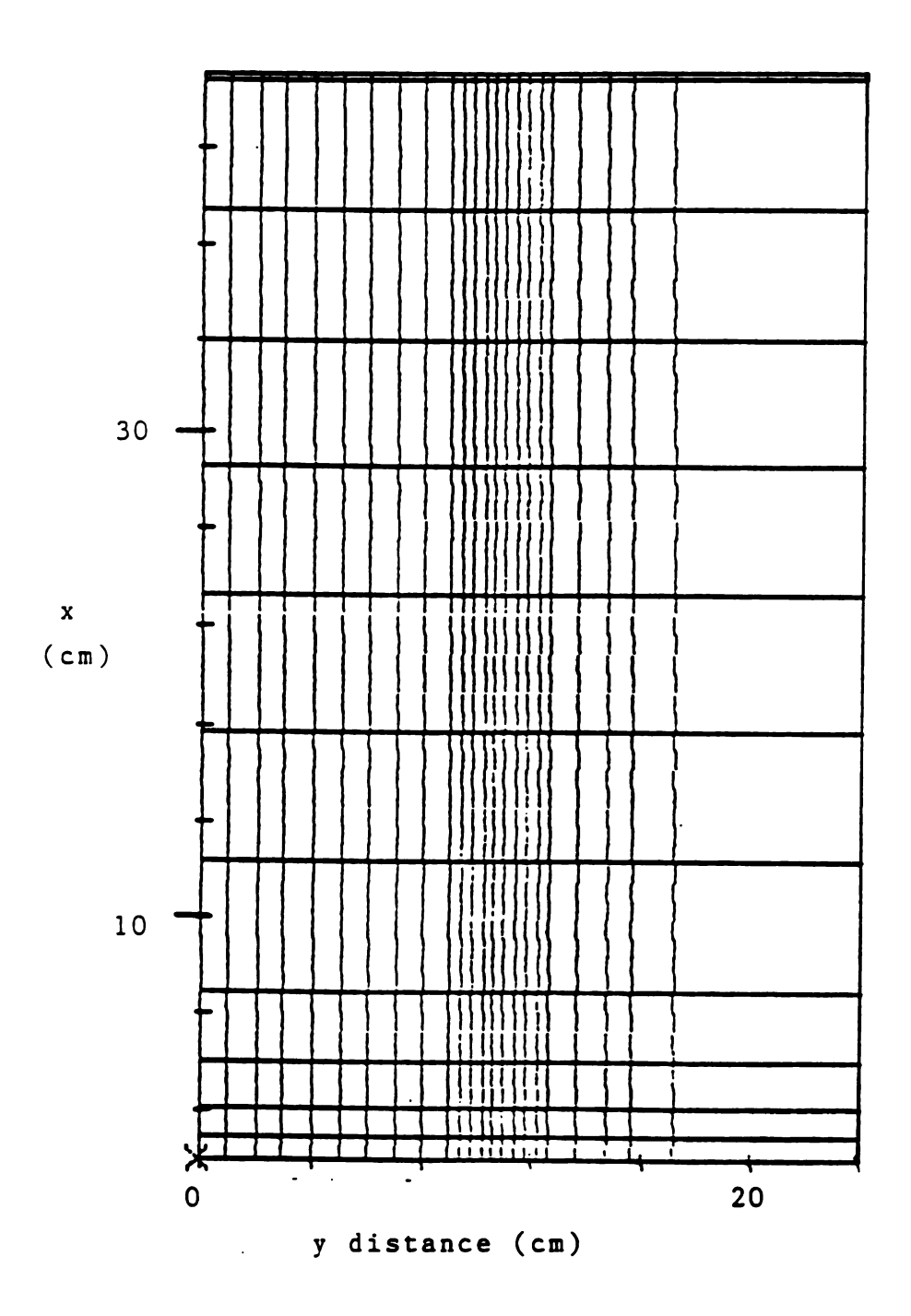


Figure 38 Measurement grid for d/w=5

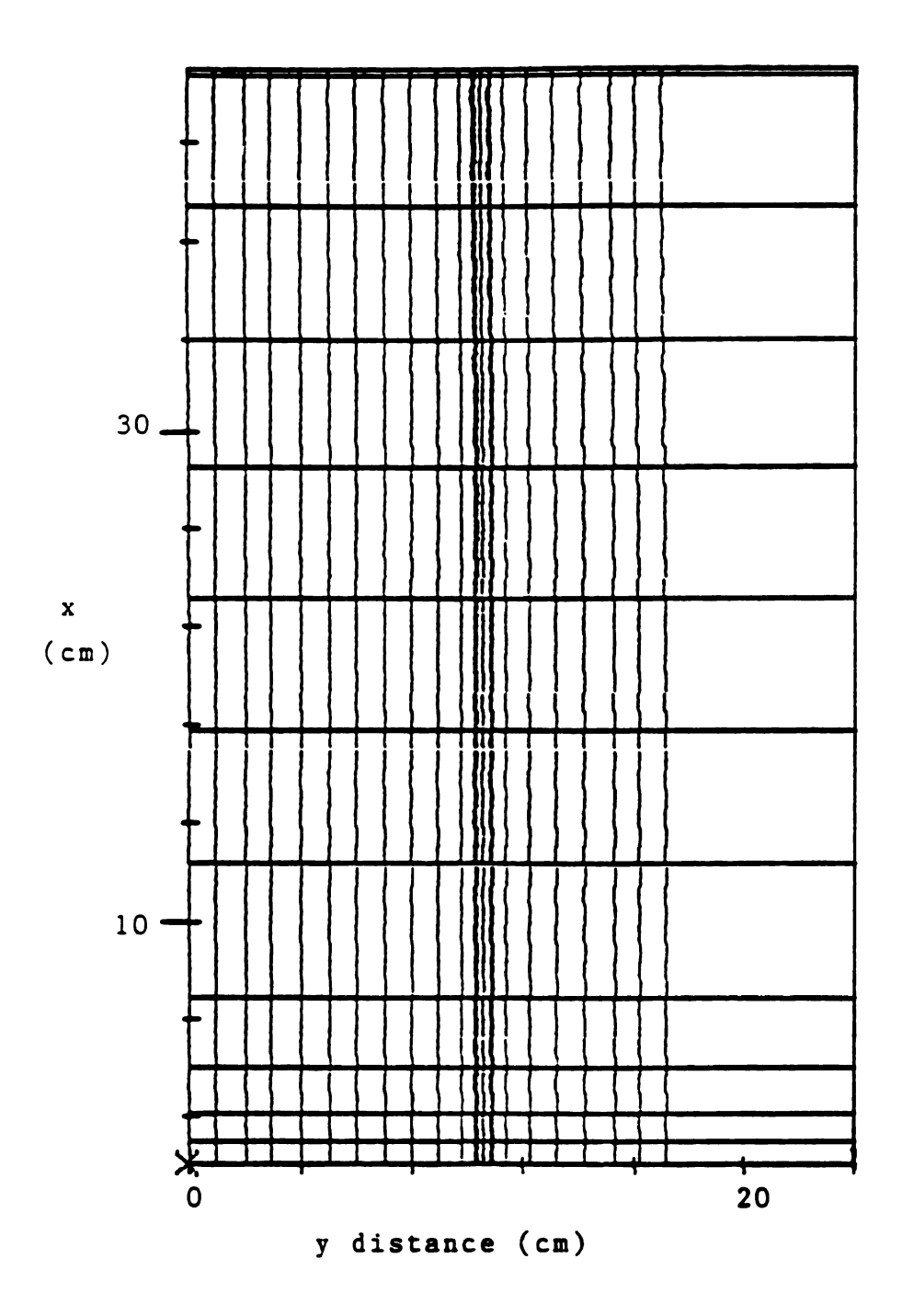


Figure 39 Measurement grid for d/w=10

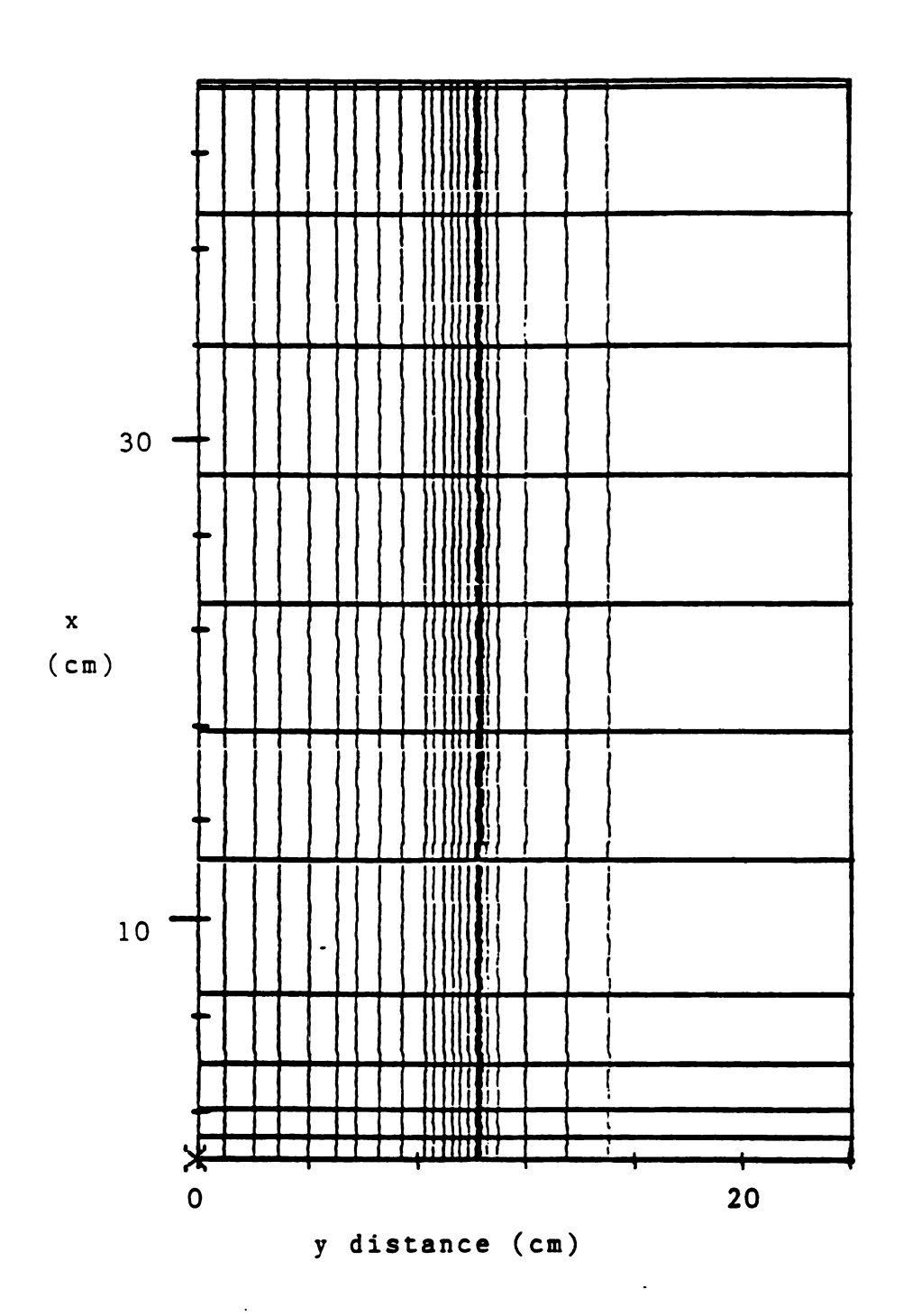


Figure 40 Measurement grid for d/w=20

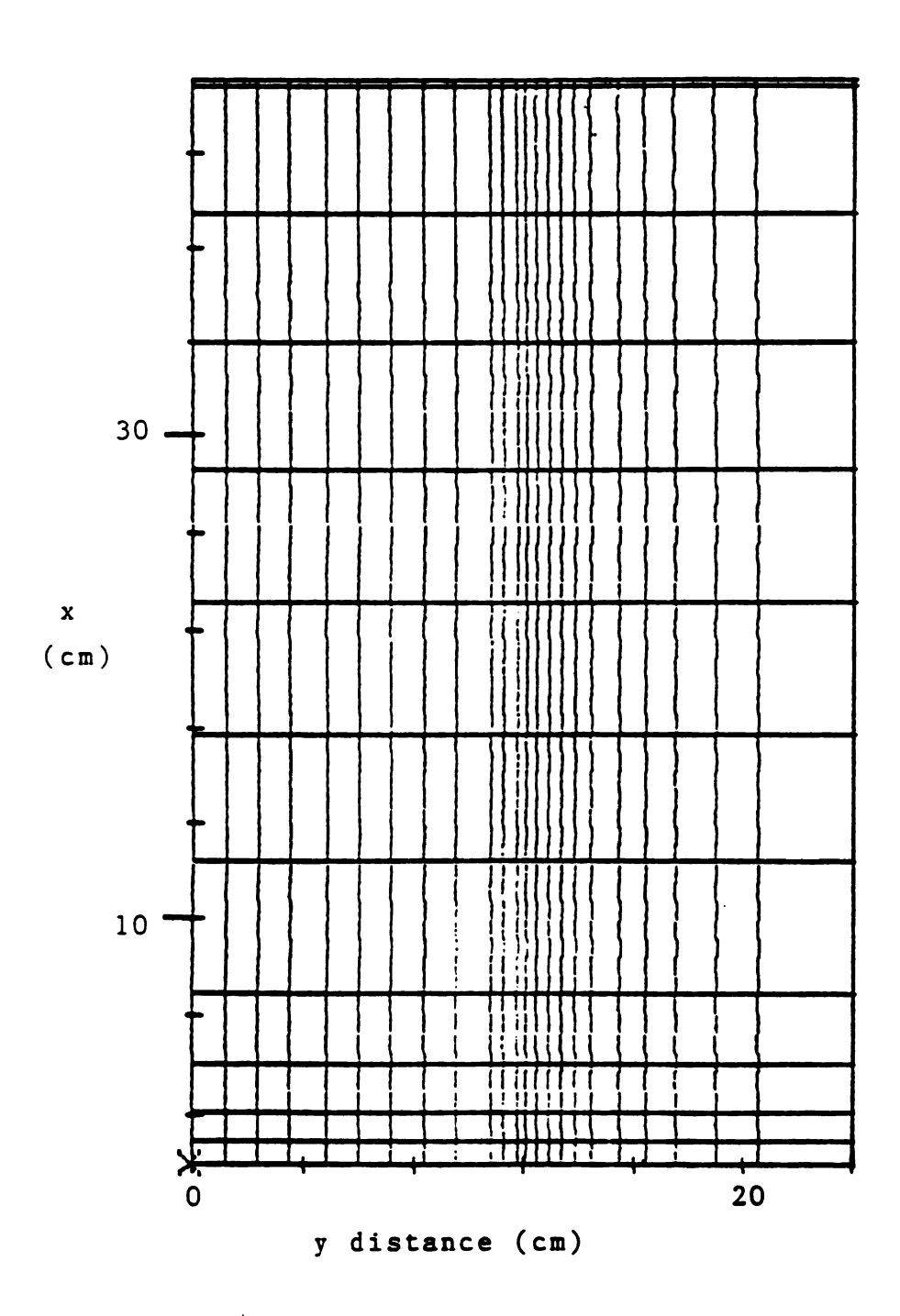


Figure 41 Measurement grid for jet issuing at 15° angle

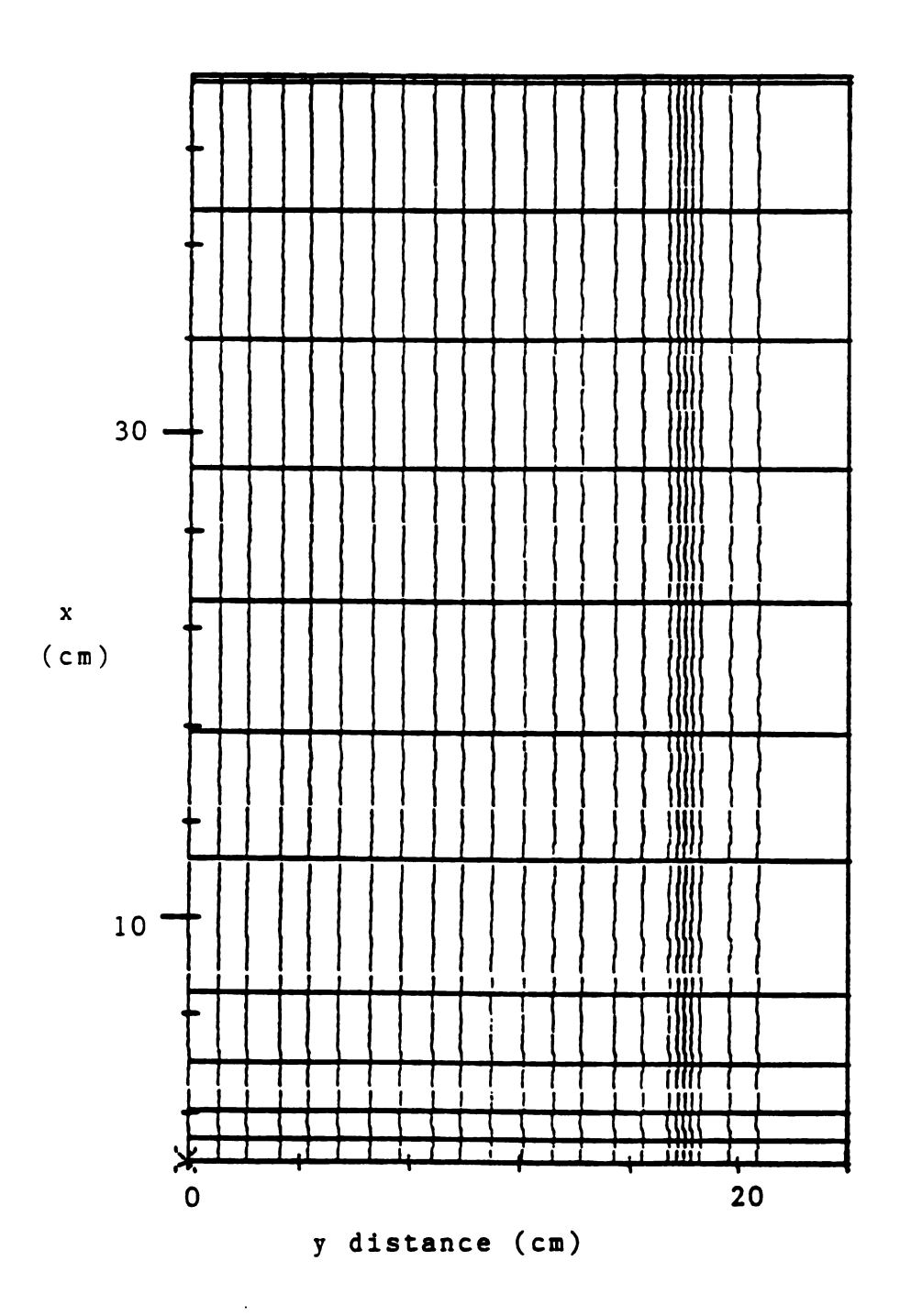


Figure 42 Measurement grid for d/w=17.5

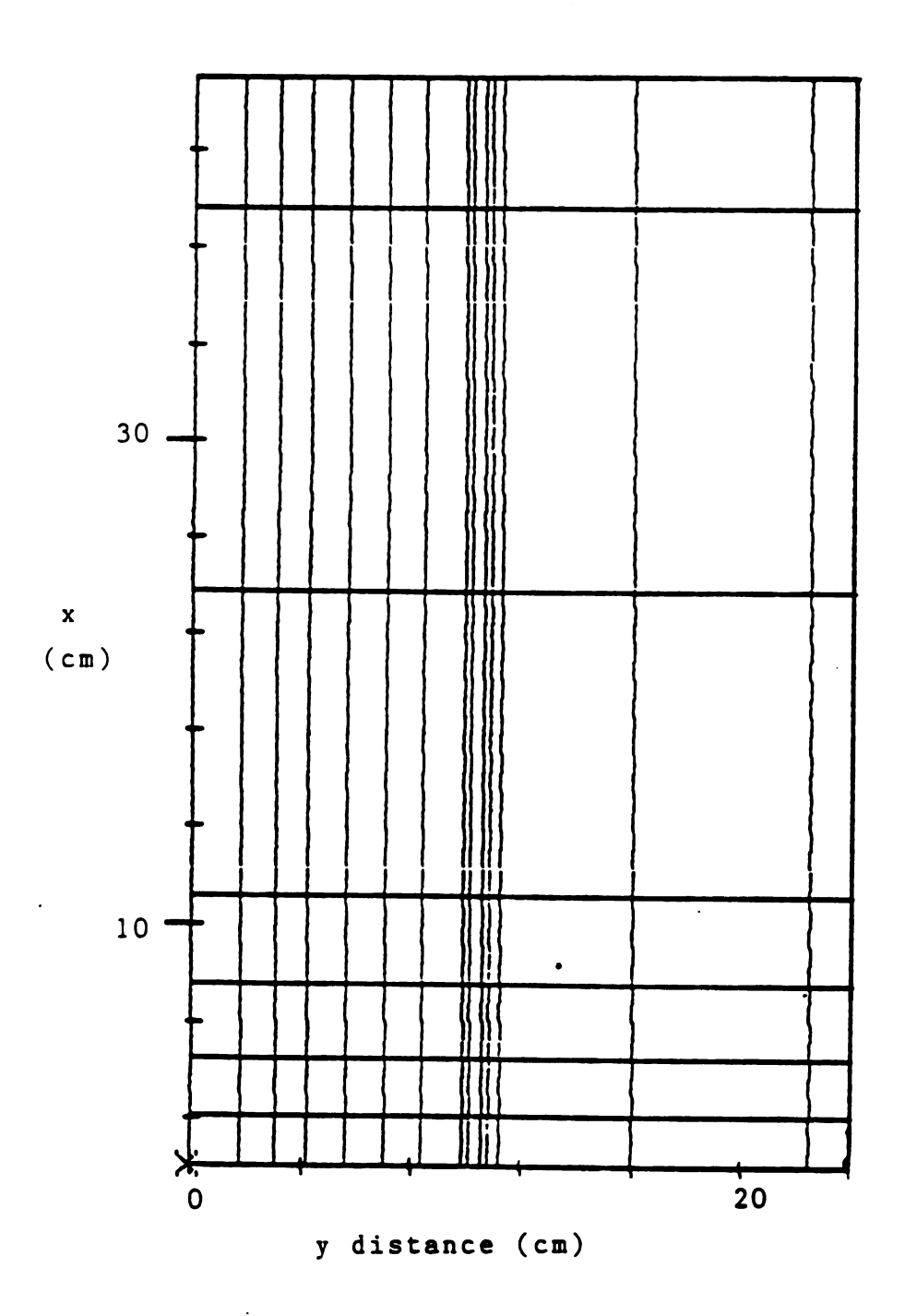


Figure 44 Course computational grid

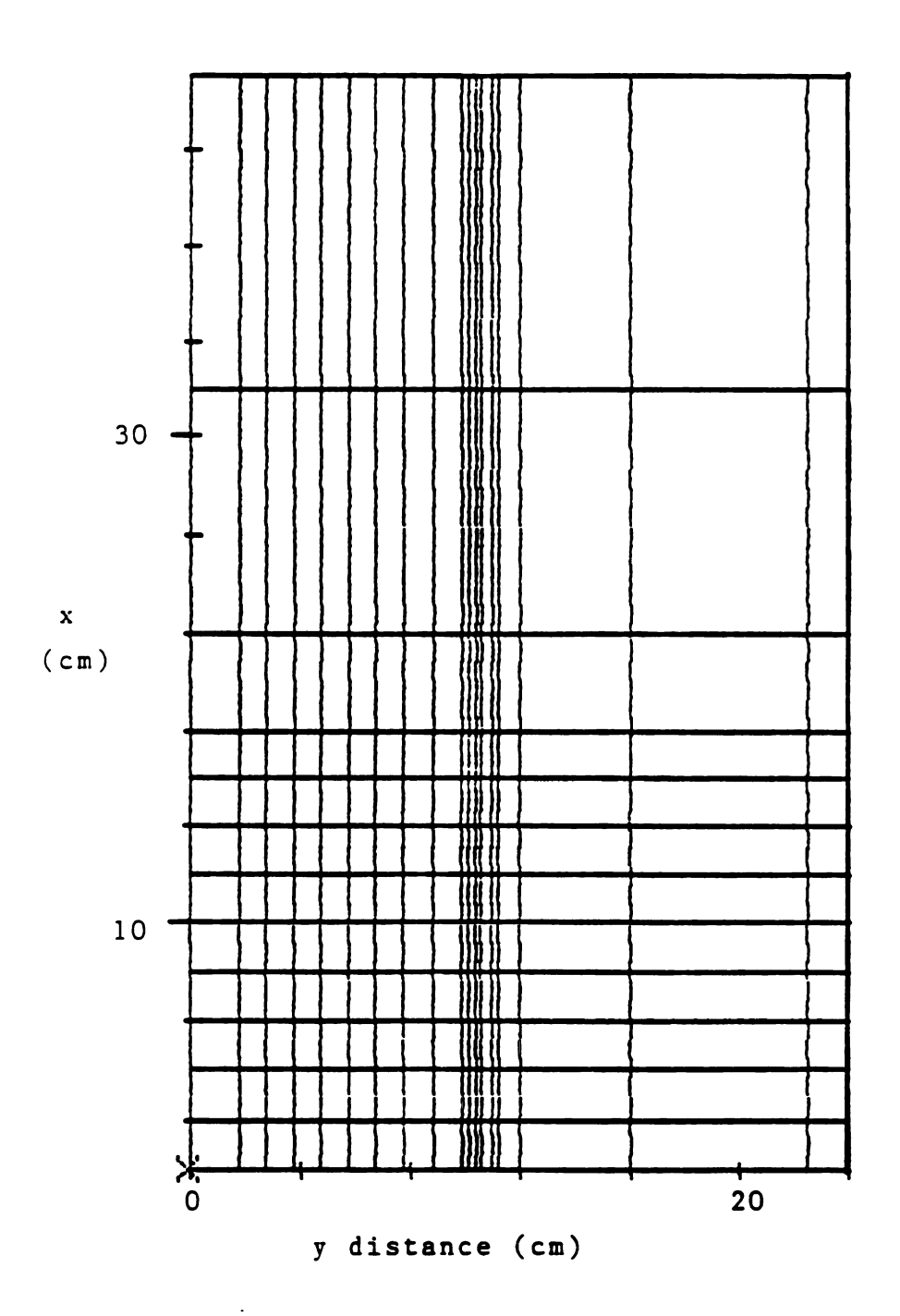


Figure 45 Fine computational grid

APPENDIX B

Table 5 Inlet velocity profiles

Number	Position along jet	d/w	Re	T _i (°C)
1	1/2	5	7600	27
2	1/2	10	3800	27
3	1/2	10	2500	27
4	1/2	20	2000	27
5	1/2	20	1300	27
6	1/2	35	1300	27
10	1/2	17.5	3800	27
11	1/2	35	2000	27
12	1/4	10	3800	27
13	1/4	10	2500	27
14	3/4	10	3800	27
15	3/4	10	2500	27

Table 6 Two dimensional checks for velocity and temperature

Position along along jet	Height above inlet (cm)	Re	T _i (°C)
1/4	0.2	3800	27
1/4	10	3800	27
1/4	40	3800	27
1/2	0.2	2500	27
1/2	10	2500	27
1/2	40	2500	27
1/2	0.2	3800	27
1/2	10	3800	27
1/2	40	3800	27
3/4	0.2	2500	27
3/4	10	2500	27
3/4	40	2500	27
3/4	0.2	3800	27
3/4	10	3800	27
3/4	40	3800	27

Table 7 Measurements at grid points

Run #	d (mm)	w (mm)	T _i (°C)	Re	Wall Setting (°C)
1	100	10	27.8	3813	10
2	100	10	38.7	3599	10
3	100	10	38.6	2494	10
4	100	10	26.8	3838	10
5	100	10	27.1	2072	10
6	100	10	26.4	1191	10
7	100	5	27.4	2022	10
8	100	10	41.6	3608	10
9	175	5	37.9	3600	10
10	175	10	38.2	2128	10
11	175	5	38.4	1914	10
12	175	5	27.5	1999	10
13	175	10	27.0	2062	10
14	175	10	27.2	3755	10
15	175	10	38.1	3622	5
16	175	10	38.6	3688	OFF
17*	100	10	27.3	3824	10
18*	100	10	26.8	2538	10
19*	100	10	38.6	3698	10
20*	100	10	38.0	2482	10

^{*-} Jet issued at 15° angle

Table 7 (continued)

Run #	d (mm)	w (mm)	T _i (°C)	Re	Wall Setting (°C)
21	100	10	27.6	2600	10
22	100	5	26.5	1330	10
23	100	5	37.9	1962	10
24	175	10	38.7	2330	10
25	175	10	27.2	2530	10
26	175	5	26.7	1307	10
27	100	20	27.4	7648	10
28	100	20	27.5	5266	10
29	100	20	37.9	4935	10
30	100	20	37.6	7069	10
31	100	20	27.4	7623	OFF
32	100	20	27.0	5306	OFF
33	100	10	27.1	3874	OFF
34	100	10	27.3	2423	OFF
35	100	5	26.5	2025	OFF
36	100	5	26.8	1329	OFF
37	175	5	27.2	1445	OFF
38	175	5	27.0	1956	OFF
39	175	10	26.9	3832	OFF

Table 8 Wall jet velocity and temperature measurements

Height (m)	d/w	T _i (°C)	Re	Wall setting
1.5	10	27	3800	ON
1.5	10	27	3800	OFF
1.5	10	27	2500	ON
1.5	10	27	2500	OFF
2.0	10	27	3800	ON
2.0	10	27	3800	OFF
2.0	10	27	2500	ON
2.0	10	27	2500	OFF
2.5	10	27	3800	ON
2.5	10	27	3800	OFF
2.5	10	27	2500	ON
2.5	10	27	2500	OFF
3.0	10	27	3800	ON
3.0	10	27	3800	OFF
3.0	10	27	2500	ON
3.0	10	27	2500	OFF

LIST OF REFERENCES

REFERENCES

- /1/ Bourque, C. and Newman, B.G. "Reattachment of a Two-Dimensional Incompressible Jet to an Adjacent Flat Plate". The Aeronautical Ouarterly, vol. XI, August 1960, pp. 201-232.
- /2/ Sawyer, R.A., "The Flow Due to a Two-Dimensional Jet Issuing Parallel to a Flat Plate" <u>Journal of Fluid Mechanics</u>, vol. 9 (1960) pp.543-560.
- /3/ Sawyer, R.A., "Two-Dimensional Reattaching Jet Flows Including the Effects of Curvature on Entrainment", <u>Journal of Fluid Mechanics</u>, vol. 17, pp481-498.
- /4/ Regenscheit, B. <u>Isotherme Luftstrahlen Klima- und Kälteing.</u>, extra 12, Published by C.F. Müller, Karlsruhe, W. Germany, 1981, pp. 138-150.
- /5/ Willie, R. and Fernholz, H. "Report on the First European Mechanics Colloquium on the Coanda Effect", <u>Journal of Fluid Mechanics</u>, vol. 23 (1965), pp. 801-819.
- /6/ Castro, I.P. and Bradshaw, P., "The Turbulent Structure of a Highly Curved Mixing Layer", <u>Journal of Fluid Mechanics</u>, vol. 73 (1976), pp. 263-304.
- /7/ Gibson, M.M., Verriopoulos, C.A. and Nagano, Y.
 "Measurements in a Heated Turbulent Boundary Layer on a
 Mildly Curved Convex Surface", Third International
 Symposium on Turbulent Shear Flows, Davis Ca., 1982.

- /8/ Abbott, D.E. and Kline, S.J., "Experimental Investigation of Subsonic Turbulent Flow Over Single and Double Backward Facing Steps." <u>Journal of Basic Engineering</u>, Trans. ASME, Sept. 1962, pp. 317-325.
- /9/ Eaton, J.K. and Johnston, J.P. "A Review of Research on Subsonic Turbulent Flow Reattachment", <u>AIAA Journal</u>, vol. 19, No. 9, Sept. 1981, pp. 1093-1100.
- /10/ Aung, W. and Goldstein, R.J. "Heat Transfer in Turbulent Separated Flow Downstream of a Rearward-Facing Step",

 <u>Israel Journal of Technology</u>, vol. 10, 1972, pp. 35-41.
- /11/ Vogel, J.C. and Eaton, J.K. "Combined Heat Transfer and Fluid Dynamic Measurements Downstream of a Backward-Facing Step", ASME Journal of Heat Transfer, vol. 107, 1985, pp. 922-929.
- /12/ Seki, N., Fukusako, S. and Hirato, T. "Turbulent Fluctuations and Heat Transfer for Separated Flow Associated with a Double Step at Entrance to an Enlarged Flat Duct", ASME Journal of Heat Transfer, Nov. 1976, pp. 588-93.
- /13/ Lamb, J.P. "Convective Heat Transfer Correlations for Planar, Supersonic, Separated Flows", ASME Journal of Heat Transfer, vol. 102, 1980, pp. 351-56.
- /14/ Aung, W, "An Experimental Study of Laminar Heat Transfer Downstream of Backsteps", ASME Journal of Heat Transfer, vol. 105, 1983, pp. 823-829.

- /15/ Gooray, A.M., Watkins, C.B. and Aung, W. "Turbulent Heat Transfer Computations for Rearward-Facing Steps and Sudden Pipe Expansions", <u>ASME Journal of Heat Transfer</u>, vol. 107, 1985, pp. 70-76.
- /16/ Glauert, M.B., "The Wall Jet", <u>Journal of Fluid</u>
 <u>Mechanics</u>", vol. 1, 1956, pp.625-643.
- /17/ Schwarz, W.H. and Cosart, WP. "The Two-Dimensional Turbulent Wall" <u>Journal of Fluid Mechanics</u>, vol. 10, 1961, pp. 481-495.
- /18/ Faeth, G.M. and Liburdy, J.A. "Fire Induced Plumes Along a Vertical Wall: Part I, The Turbulent, Weakly Buoyant Region". Report for U.S. Dept. of Commerce, Pennsylvania State University, 1977.
- /19/ Schmitz, R. "Berechnung Turbulenter Raumluft Strömungen bei Gekoppeltem Impuls-, Wärme- und Stoffaustausch", Doctoral Dissertation, RWTH Aachen, W. Germany, Sept. 1985.
- /20/ Pun, W.M., Spalding, D.B. "A General Computer Program for Two-Dimensional Elliptic Flows", HTS Report 76/2 Imp. College of Science and Technology, Mechanical Engineering Dept., Aug. 1977.
- /21/ Patankar, S.V. <u>Numerical Heat Transfer and Fluid Flow</u>,
 Hemisphere Publishing Corp., Washington, McGraw-Hill,
 1980.

- /22/ Bronstein, I.N. and Semendjajew, K.A. Taschenbuch Der Mathematik, Harri Deutsch, Thun, E. Germany, 1977, p.177.
- /23/ Tennekes, H. and Lumley, J.L. <u>A First Course in Turbulence</u>, MIT Press, Cambridge, Mass. 1972.
- /24/ Arpaci, V.S. and Larsen, P.S. <u>Convection Heat Transfer</u>, Prentice-Hall, Inc., Englewood Cliffs, N.J. 1984.
- /25/ Ewes, I. Studienarbeit, Lehrstuhl für Wärmeübertragung und Klimatechnik, RWTH Aachen, FRG, Aug. 1985.
- /26/ Verweyen, N. Studienarbeit, Lehrstuhl für Wärmeübertragung und Klimatechnik, RWTH Aachen, FRG, May 1983
- /27/ Eppert, V. Studienarbeit, Lehrstuhl für Warmeübertragung und Klimatechnik, RWTH Aachen, FRG, Aug. 1986.

MICHIGAN STATE UNIV. LIBRARIES
31293008236014